[redacted]

[redacted]

NACA

RESEARCH MEMORANDUM

FORCE AND PRESSURE CHARACTERISTICS FOR A SERIES OF NOSE INLETS AT MACH NUMBERS FROM 1.59 TO 1.99

III - CONICAL-SPIKE ALL-EXTERNAL-COMPRESSION INLET WITH SUPERSONIC COWL LIP

By Maynard I. Weinstein and Joseph Davids

Lewis Flight Propulsion Laboratory
Cleveland, Ohio

NATIONAL ADVISORY COMMITTEE FOR AERONAUTICS

WASHINGTON
February 14, 1951

[redacted]

[redacted]

2039

NATIONAL ADVISORY COMMITTEE FOR AERONAUTICS

RESEARCH MEMORANDUM

FORCE AND PRESSURE CHARACTERISTICS FOR A SERIES OF NOSE INLETS AT MACH NUMBERS FROM 1.59 TO 1.99

III - CONICAL-SPIKE ALL-EXTERNAL-COMPRESSION INLET WITH SUPERSONIC COWL LIP

By Maynard I. Weinstein and Joseph Davids

SUMMARY

An investigation was conducted in the NACA Lewis 8- by 6-foot supersonic wind tunnel to determine the force and pressure characteristics of an all-external compression inlet having a conical spike and a supersonic cowl lip. Measurements of lift, drag, pitching moment, and internal and external pressures were made at free-stream Mach numbers of 1.59, 1.79, and 1.99 for a range of mass-flow ratios and angles of attack to 10°. The average Reynolds number based on inlet diameter was 2,300,000.

The drag increased rapidly with decreasing mass flow as a consequence of the increase in additive drag. The drag rise due to angle of attack resulted primarily from an increase in the normal force. At zero angle of attack, adequate theoretical predictions were made of the additive drag, friction drag, and at shock-swallowed conditions, the pressure drag.

The total-pressure recovery was in general only slightly reduced by increases in angle of attack to 10°.

INTRODUCTION

A general study of the aerodynamic characteristics of a series of nose inlets suitable for supersonic ram-jet engines was conducted in the Lewis 8- by 6-foot supersonic wind tunnel. This report presents

[redacted]

the results of an investigation of a conical-spike inlet designed to give all-external compression and having a supersonic cowl lip. The performance of two other inlets is discussed in references 1 and 2. 2039

The purpose of the investigation was to obtain force, moment, and pressure data, and when possible to compare the experimental results with theory. Data were obtained for a range of mass-flow ratios and angles of attack at free-stream Mach numbers 1.59, 1.79, and 1.99. The Reynolds number based on inlet diameter varied from 2.0 to 2.4 × 10^6.

SYMBOLS

The following symbols are used in this report:

C_D drag coefficient, D/q_0S_m

C_f friction drag coefficient, based on wetted area

C_L lift coefficient, L/q_0S_m

C_M pitching-moment coefficient, about the base of the model, $G/q_0S_m l$

C_p pressure coefficient, $p-p_0/q_0$

D drag

d diameter at area of maximum cross section, 8.125 inches

G pitching moment about base of model

L lift

l length of model, 58.66 (in.)

M Mach number

m_3/m_0 mass-flow ratio, $\frac{\rho_3U_3S_3}{\rho_0U_0S_c}$

P total pressure

p static pressure

q dynamic pressure, $\gamma pM^2/2$

2039

Re Reynolds number

S area

S_c inlet capture area defined by cowl lip, 0.1674 (sq ft)

S_m maximum cross-sectional area, 0.3601 (sq ft)

U velocity

u velocity in boundary layer

v_x axial perturbation velocity

x,r,θ cylindrical coordinates

y distance from model surface

α angle of attack

γ ratio of specific heats, 1.40

δ boundary-layer thickness

ρ mass density

Subscripts:

a additive drag

f friction

l local condition in boundary layer

p pressure

δ conditions at outer edge of boundary layer

0 free stream

1 cowl lip

2 station at 7.00 inches downstream of cowl lip

3 combustion-chamber inlet

APPARATUS AND PROCEDURE

A schematic assembly of the model is shown in figure 1(a). The apparatus is similar to that employed in reference 1 except for the inlet, which is detailed in figure 1(b). The inlet was designed so that the oblique shock would intersect the cowl lip at a Mach number of 1.80. The cowl lip had a relatively sharp supersonic profile designed to be approximately tangent to the streamlines immediately behind the oblique shock at a Mach number of 1.80. 2039

Two models designated A and B were investigated. Model A had an internal contraction ratio of 1.04. With this contraction, internal choking occurred at Mach number 1.79 due to the growth of boundary layer, which prevented the normal shock from being swallowed. In order to help alleviate this condition, the spike contour of model B was slightly reduced from that of model A, as shown by the model coordinates presented in table I. In addition to the spike-contour modification, the length of the support struts was decreased $2\frac{1}{4}$ inches. The same cowl was used for both models.

Shown in figure 2 is the longitudinal variation of the ratio of the local annular area (based on an average of surface normals) to the area of the simulated combustion chamber. The aforementioned modification in spike contour and support-strut length can be seen in this figure.

The model instrumentation and the experimental techniques were similar to those described in reference 1. The location of the static-pressure orifices are given in table II. Flow stations are defined in figure 3.

The internal mass-flow rate was computed by using the average total pressure measured at the combustion-chamber inlet and assuming isentropic flow to the minimum geometric area at the tail plug where choking occurred. A correction factor of 0.97 (determined from shock-swallowed operation) was applied to all mass-flow calculations.

Data were obtained for a range of mass flows and at angles of attack from 0° to 10°. Pressure data were obtained at Mach numbers 1.79 and 1.99 using model A. Force and moment characteristics were determined at Mach number 1.79 with model A and at Mach numbers 1.59, 1.79, and 1.99 with model B.

2039

RESULTS AND DISCUSSION

External-Flow Characteristics

Zero angle of attack. - The variation of total drag coefficient C_D with mass-flow ratio m_3/m_0 for model B is presented in figure 4 for the three Mach numbers of the investigation. Unless otherwise noted, all external-pressure data are presented for model A and all force data for model B. The drag represents all the forces external to the entering stream tube and the model shell.

With decreasing mass-flow ratio, the drag coefficient increased rapidly at a rate that increased slightly with free-stream Mach number. The increase in drag coefficient at critical mass-flow ratio with decreasing Mach number, shown in figure 5, was in part due to the increased spillage that accompanied a decrease in the Mach number.

External and internal pressure distributions are presented in tabular form in tables III to V. The longitudinal external-pressure distribution for a range of mass-flow ratios at Mach numbers 1.79 and 1.99 is shown in figure 6. Expansion of the flow around the inlet increased with increasing mass spillage. The most pronounced variations of pressures extended only approximately 2 diameters downstream of the lip.

The decrease in pressure coefficient at $x/d \cong 4.00$ was caused by expansion of the flow as a result of the change in model contour from a conical to a cylindrical section. At $x/d \cong 1.22$ the decrease was the result of the joint between the cowl and the afterbody, whereas at $M_0 = 1.99$ the decrease in pressure coefficient for $x/d \cong 3.25$ resulted from a weak tunnel disturbance. Close agreement with linearized potential theory (valid only for shock-swallowed conditions) is shown for $m_3/m_0 = 1.0$ at $M_0 = 1.99$ and for $m_3/m_0 = 0.940$ at $M_0 = 1.79$. The theoretical computations neglected the influence of the bow shock at the cowl lip, inasmuch as the region affected was of extremely limited extent relative to the model length.

The pressure drag coefficient $C_{D,p}$, evaluated from an integration of the external pressures at various mass-flow ratios, is presented in figure 7. The reduction of cowl pressures with increasing spillage resulted in an actual thrust force at mass-flow ratios less than approximately 0.70. Comparison of the experimental and theoretical pressure drags shows good agreement at $M_0 = 1.99$ for $m_3/m_0 = 1.0$. Extrapolation to $m_3/m_0 = 1.0$ for data at $M_0 = 1.79$ also indicates good agreement with theory.

Typical radial distributions of local Mach number, measured by the boundary-layer rake at station 51.03, are shown in figure 8 for a range of mass-flow ratios at free-stream Mach numbers of 1.79 and 1.99. The Mach numbers were calculated from the Rayleigh equation by assuming adiabatic flow at free-stream total temperature and uniform radial static pressure at the measured surface value. Local Mach numbers greater than free stream were a consequence of surface static pressures at the rake that were slightly less than ambient (fig. 6). As discussed in reference 3, the form of the profiles and their displacement with mass-flow variation is associated with the total-pressure losses due to flow through the bow shock wave. The method of reference 3 was employed to isolate the bow shock losses from the total losses measured at the individual rake tubes. The boundary-layer thicknesses δ were consequently determined to extend to the rapid change in slope of the profiles (shown by arrows in fig. 8). For these values of δ, the dimensionless velocity profiles are shown in figure 9 to vary according to the 1/7 power law.

Calculation of the decrement of momentum in the boundary layer yielded the friction drag coefficient, which is shown in figure 10 to be essentially independent of mass flow and free-stream Mach number. Good agreement is indicated in figure 11 between the average value of skin friction coefficient of 0.0018 (based on wetted area) and the von Kármán turbulent compressible theory for flat plates (reference 4). Indicated Reynolds numbers are based on free-stream conditions and the length of the external model shell ahead of the rake.

The variation of additive-drag coefficient with mass-flow ratio is shown in figure 12. Additive drag was obtained from a momentum balance (applied to the flow between flow stations 0 and 2), which included the contribution of the measured pressures along the spike and the cowl. The momentum at station 2 was obtained from the corrected mass flow and the measured static pressure. The additive drag increased rapidly with decreasing mass-flow ratio and increased slightly with Mach number at a given mass-flow ratio. The slightly negative values at $m_3/m_0 = 1.0$ for $M_0 = 1.99$ may be partly ascribed to a neglect of viscous effects. Excellent agreement was obtained with the one-dimensional theory of reference 5.

The sum of the drag components evaluated from the pressure data of model A is compared in figure 13 with the total drag obtained from force measurements of model A and B at $M_0 = 1.79$ and of model B at $M_0 = 1.99$. The friction drag was modified from the value given in figure 10 to account for the model length downstream of the boundary-layer rake. Good agreement is shown for model A at $M_0 = 1.79$. At $M_0 = 1.99$ the measured drag of model B was less than the summarized

-2049 component drags of model A. Because model A exhibited greater drag values than did model B at $M_0 = 1.79$, however, it is presumed that good agreement would result at $M_0 = 1.99$ from comparison of the same model. Figure 13 shows that for either model the additive drag was directly responsible for the rapid increase in drag with increasing mass-flow spillage.

Angle of attack. - The variation of total drag coefficient with mass-flow ratio is shown in figure 14 for angles of attack to 10°. The rate of drag increase with increasing mass flow spillage was essentially independent of angle of attack. As discussed in references 1 and 2, the increase in drag at a given mass-flow ratio resulted from the increase in normal force while the axial force remained relatively constant.

The lift and-pitching moment coefficients (which include the additive components due to mass spillage) are presented as a function of mass-flow ratio for various angles of attack in figures 15 and 16, respectively. For the determination of the pitching moment, the force on the model due to the inlet flow deflection was assumed to act at the cowl lip. The lift and pitching-moment coefficients decreased slightly with decreasing mass-flow ratio. At a given mass-flow ratio and angle of attack, the lift coefficient increased slightly with free-stream Mach number but the moment coefficient remained approximately constant. The location of the center of pressure (fig. 17) varied between approximately 4.25 and 5.25 diameters ahead of the base.

At critical mass-flow ratios, the drag, drag increment, lift, and pitching moment varied with angle of attack as shown in figure 18. As in references 1 and 2, the modified theory of reference 6 is in good agreement for the moment coefficient at low angles of attack but underestimates the drag increments and lift coefficients.

The effect of angle of attack on the longitudinal pressure distribution is illustrated in figure 19 for Mach number 1.79. Additional data are presented in tables III to V. The decrease in upper-surface pressures with increasing angle of attack extended approximately 2 diameters downstream of the cowl lip. The simultaneous increase in lower-surface pressures extended the length of the model.

Internal-Flow Characteristics

Zero angle of attack. - The variation of total-pressure recovery P_3/P_0 and combustion-chamber Mach number M_3 with mass-flow ratio is shown in figure 20. The total pressure P_3 is presented as the corrected value based on the corrected mass flow and the average static pressure at the rake station rather than the slightly greater value indicated by the combustion-chamber survey rake. Combustion-chamber Mach number M_3 was computed assuming isentropic expansion from the annular area at flow station 3 to the area of the combustion chamber with the sting removed. At Mach number 1.59 the subcritical total-pressure recovery was invariant with mass-flow ratio, whereas at Mach numbers 1.79 and 1.99 the recovery decreased with decreasing mass-flow ratio. Maximum total-pressure recoveries of 90, 87, and 79 percent were obtained at Mach numbers of 1.59, 1.79, and 1.99, respectively. 2039

The components of the over-all total-pressure loss are presented in figure 21 as the inlet losses $\Delta P_{0-2}/P_0$ and the subsonic-diffuser losses $\Delta P_{2-3}/P_0$. The average total pressure P_2 at flow station 2 was computed from the corrected mass flow and local static pressure. Decreasing the mass-flow ratio decreased the losses in the subsonic diffuser but increased the inlet losses.

A comparison of the measured subcritical inlet total-pressure recovery P_2/P_0 and the calculated recovery, the latter determined as in reference 1, is presented in figure 22. The calculated pressure recoveries were approximately 5 percent greater than the measured values. Good agreement can be seen in the slope of the measured and calculated values.

As shown in figure 23, the total-pressure recovery P_3/P_2 of the subsonic diffuser for subcritical mass-flow ratios was relatively independent of Mach number but decreased with increasing mass-flow ratio to approximately 94 percent at critical mass-flow ratios. A large part of this decrease is attributable to the wake effects of the support struts.

Mach number profiles at the combustion-chamber inlet are shown in figure 24 for $M_0 = 1.79$. The Mach number variation increased and the peak velocity moved toward the outer shell as the mass-flow ratio increased. The differences in profiles of adjacent rakes was a consequence of the support-strut wake effects.

<u>Angle of attack.</u> - The effect of angle of attack on the subcritical total-pressure recovery and combustion-chamber Mach number was negligible at $M_0 = 1.59$ (fig. 25). Slight reductions in pressure recovery occurred at an angle of attack of 10° for $M_0 = 1.79$ and at 6° and 10° for $M_0 = 1.99$. Flow instability occurred at 10° for $M_0 = 1.99$ for mass-flow ratios less than 0.84. Due to the intensity of the instability, no data were taken in this region.

2039

The decrease in maximum mass-flow ratio with angle of attack was greater at an angle of attack of 10° than that attributable to the area reduction which occurs when the inlet area is multiplied by the cosine of α. This mass-flow limitation presumably resulted from premature choking in the upper portion of the subsonic diffuser near the leading edge of the support struts (reference 1).

The inlet and subsonic diffuser components of the over-all total-pressure loss are shown in figure 26 to be essentially independent of angle of attack at $M_0 = 1.79$. The minor discrepancy between these data and the pressure recovery at 10° angle of attack (fig. 25(b)) is attributable to the slight differences between models A and B.

Increasing the angle of attack to 10° resulted in relatively greater total pressure and mass flow in the upper portion of the subsonic diffuser and possible flow separation from the lower diffuser surface. These effects were also noted in references 1 and 2.

SUMMARY OF RESULTS

An investigation was conducted at Mach numbers 1.59, 1.79, and 1.99 to determine the force, moment, and pressure characteristics of an all-external compression, conical spike inlet having a supersonic cowl lip. The following results were obtained at an average Reynolds number of 2,300,000 (based on inlet diameter) for a range of mass flows and angles of attack to 10°:

1. The rapid increase in drag coefficient with decreasing mass flow and the increase in minimum drag with decreasing Mach number was associated with the increase in additive drag. The drag rise due to angle of attack resulted primarily from an increase in the normal force; the axial force remained relatively constant.

2. The variation of additive drag with mass-flow ratio was satisfactorily calculated from a momentum balance and assuming one-dimensional flow.

3. At zero angle of attack and with no mass spillage, the external pressure distribution and hence the pressure drag were satisfactorily predicted by linearized potential theory.

4. The friction drag was independent of Mach number and mass flow and agreed well with the value predicted by the theory for turbulent compressible flow over a flat plate. 2039

5. The total-pressure recovery was in general only slightly reduced by increases in angle of attack.

Lewis Flight Propulsion Laboratory,
National Advisory Committee for Aeronautics,
Cleveland, Ohio.

2039

REFERENCES

1. Esenwein, Fred T., and Valerino, Alfred S.: Force and Pressure Characteristics for a Series of Nose Inlets at Mach Numbers from 1.59 to 1.99. I - Conical-Spike All-External Compression Inlet with Subsonic Cowl Lip. NACA RM E50J26, 1951.

2. Obery, L. J., and Englert, G. W.: Force and Pressure Characteristics for a Series of Nose Inlets at Mach Numbers from 1.59 to 1.99. II - Isentropic-Spike All-External Compression Inlet. NACA RM E50J26a, 1951.

3. Luidens, Roger W., and Madden, Robert T.: Interpretation of Boundary-Layer Pressure-Rake Data in Flow with a Detached Shock. NACA RM E50I29a, 1950.

4. de Kármán, Th.: The Problem of Resistance in Compressible Fluids. Quinto Convegno "Volta", Reale Accademia d'Italia (Roma), Sett. 30-Ott. 6, 1935, pp. 3-57.

5. Dailey, C. L., and Mc Farland, H. W.: Development of Ramjet Components. Prog. Rep. 9961-8, Univ. Southern Calif. Aero. Lab., USCLA, Feb. 7, 1950. (Bi-Monthly Prog. Rep. Dec. 1949-Jan. 1950 under Navy Contract N)a(s) 9961.)

6. Allen, H. Julian: Estimation of the Forces and Moments Acting on Inclined Bodies of Revolution of High Fineness Ratio. NACA RM A9I26, 1949.

TABLE I - TABLES OF COORDINATES FOR 8-INCH RAM-JET CONFIGURATION

2039

(a) Center body coordinates

Station (in.)	Diameter (in.)	
	Model A	Model B
0.378	2.800	2.800
.500	2.890	2.875
1.000	3.125	3.080
1.500	3.295	3.255
2.000	3.448	3.413
2.500	3.593	3.555
3.000	3.730	3.638
3.500	3.860	3.815
4.000	3.980	3.935
4.500	4.090	4.045
5.000	4.193	4.153
6.000	4.382	4.340
7.000	4.533	4.495
7.750	4.600	4.585
7.910	4.600	4.600
10.000	4.585	4.585
12.000	4.545	4.545
14.000	4.486	4.486
16.000	4.415	4.415
18.000	4.327	4.327
20.000	4.220	4.220
22.000	4.084	4.084
24.000	3.922	3.922
26.000	3.715	3.715
30.030	3.343	3.343

(b) Outer shell coordinates

Station	External diameter (in.)	Internal diameter (in.)
0.250	5.660	5.560
.500	5.740	5.615
.750	5.823	5.665
1.000	5.890	5.715
1.500	6.017	5.809
2.000	6.128	5.897
2.500	6.227	5.981
3.000	6.312	6.062
4.000	6.464	6.214
5.000	6.603	6.353
6.000	6.728	6.478
7.000	6.828	6.578
8.000	6.900	6.650
8.375	6.920	6.670
9.905	6.998	6.748
22.000	7.616	7.366
30.000	8.024	7.774
32.000	8.125	7.875
56.000	8.125	7.875

NACA

2039

TABLE II - LOCATION OF STATIC-PRESSURE ORIFICES FOR PRESSURE MODEL

(a) Location of static tubes along shell contour

Station		
[a]External		[b]Internal
0.500	11.000	0.500
1.000	12.000	1.000
1.500	14.000	1.500
2.000	16.000	2.000
2.500	18.000	2.500
3.000	21.000	3.000
4.000	24.000	4.000
5.000	27.000	5.000
6.000	31.000	6.000
7.000	35.000	7.000
8.000	40.000	8.000
9.000	45.000	9.000
10.000		

(b) Location of static tubes ($\theta = 0^\circ$)

Station	
Spike	Island
-1.00	8.00
-0.50	9.00
0	10.00
0.50	11.00
1.00	12.00
1.50	14.00
2.00	16.00
2.50	18.00
3.00	21.00
4.00	24.00
5.00	27.00
6.00	31.00
7.00	37.00

[a]Two rows of orifices at $\theta = 180^\circ$ and $\theta = 270^\circ$.

[b]$\theta = 0^\circ$.

TABLE III - EXTERNAL AND INTERNAL PRESSURE COEFFICIENTS OF NACA 8-INCH RAM-JET CONFIGURATION FOR FOUR ANGLES OF ATTACK AT FREE-STREAM MACH NUMBER OF 1.79

(a) Longitudinal distribution of C_p.

Station	$\alpha = 0^\circ$; $m_3/m_0 = 0.940$				$\alpha = 0^\circ$; $m_3/m_0 = 0.892$				$\alpha = 0^\circ$; $m_3/m_0 = 0.765$				$\alpha = 0^\circ$; $m_3/m_0 = 0.527$				$\alpha = 0^\circ$; $m_3/m_0 = 0.300$			
	Outer shell			Center body	Outer shell			Center body	Outer shell			Center body	Outer shell			Center body	Outer shell			Center body
	External		Internal		External		Internal		External		Internal		External		Internal		External		Internal	
θ →	180°	270°	0°	0°	180°	270°	0°	0°	180°	270°	0°	0°	180°	270°	0°	0°	180°	270°	0°	0°
-1.0				0.504				0.500				0.596				1.267				1.364
-0.5				.512				.546				1.220				1.324				1.430
0				.517				1.169				1.246				1.386				1.412
0.5	0.219	0.203	1.112	.830	0.128	0.116	1.255	.947	0.001	-0.014	1.383	1.119	-0.199	-0.219	1.540	1.357	-0.298	-0.303	1.629	1.535
1.0	.169	.152	1.057	.980	.134	.115	1.213	1.134	.066	.062	1.350	1.278	-.067	-.080	1.512	1.469	-.190	-.213	1.611	1.590
1.5	.131	.120	1.064	1.029	.109	.096	1.216	1.182	.068	.056	1.348	1.322	-.024	-.054	1.510	1.497	-.110	-.116	1.607	1.603
2.0		.090	1.065	1.039		.074	1.211	1.198		.045	1.345	1.335		-.021	1.507	1.505		-.084	1.605	1.607
2.5	.067	.078	1.044	1.055	.096	.066	1.208	1.198	.064	.045	1.344	1.337	.012	-.005	1.507	1.508	-.045	-.057	1.606	1.607
3.0		.065	1.042	1.050		.054	1.208	1.198		.034	1.344	1.337		-.005	1.508	1.508		-.047	1.606	1.607
4.0	.048	.040	1.036	1.039	.036	.035	1.206	1.206	.022	.019	1.344	1.344	-.006	-.005	1.508	1.512	-.032	-.039	1.606	1.607
5.0	.036	.025	1.003	1.008	.026	.020	1.195	1.192	.012	.008	1.339	1.339	-.009	-.014	1.507	1.510	-.028	-.034	1.606	1.607
6.0	.018	.008	.964	.937	.010	.004	1.183	1.162	-.001	-.006	1.335	1.319	-.018	-.023	1.507	1.509	-.032	-.036	1.605	1.604
7.0		-.004	.892	.892		-.005	1.157	1.150		-.016	1.319	1.316		-.029	1.500	1.500		-.040	1.603	1.604
8.0	.004	-.004	.922	.895	-.002	-.005	1.166	1.142	-.010	-.013	1.326	1.308	-.023	-.025	1.503	1.497	-.032	-.034	1.604	1.603
9.0	-.003	-.010	.861	.900	-.005	-.012	1.143	1.166	-.013	-.020	1.313	1.326	-.024	-.029	1.500	1.508	-.029	-.036	1.603	1.606
10.0	-.009	-.015		.807	-.012	-.018		1.160	-.018	-.023		1.326	-.028	-.033		1.510	-.034	-.037		1.607
11.0	-.004	-.010		.612	-.007	-.012		1.180	-.013	-.018		1.159	-.024	-.025		1.513	-.029	-.031		1.608
12.0	0	-.001		.918	-.003	-.006		1.221	-.009	-.010		1.361	-.020	-.018		1.520	-.026	-.022		1.609
14.0	0	.004		1.092	-.003	0		1.298	-.007	-.004		1.407	-.016	-.012		1.539	-.020	-.016		1.615
16.0	-.002	.005		1.198	-.006	-.003		1.353	-.010	-.006		1.446	-.014	-.010		1.557	-.018	-.011		1.621
18.0	.005	.003		1.276	.003	-.001		1.399	-.001	-.004		1.477	-.007	-.007		1.570	-.008	-.010		1.626
21.0	.008	.004		1.377	.007	0		1.462	.004	-.003		1.519	-.002	-.005		1.591	-.003	-.008		1.633
24.0	.001	.008		1.459	.011	.006		1.516	.009	.003		1.553	.004	0		1.609	.004	-.001		1.639
27.0	.006	.010		1.514	.005	.008		1.556	.004	.006		1.581	-.001	-.004		1.621	-.002	-.003		1.645
31.0	.007			1.555	.005			1.582	.004			1.596	.003			1.630	.003			1.647
35.0	-.016				-.016				-.017				-.018				-.018			
37.0				1.594				1.620				1.625				1.639				1.648
40.0	-.010				-.009				-.010				-.012				-.011			
45.0	-.013				-.012				-.013				-.014				-.014			

(b) Circumferential distribution of C_p.

Station	Outer shell, external				Outer shell, external				Outer shell, external				Outer shell, external				Outer shell, external			
θ →	198°	216°	234°	252°	198°	216°	234°	252°	198°	216°	234°	252°	198°	216°	234°	252°	198°	216°	234°	252°
0.5	0.230	0.237	0.230	0.215	0.146	0.149	0.142	0.127	0.014	0.017	0.012	-0.002	-0.183	-0.178	-0.177	-0.209	-0.294	-0.291	-0.291	-0.301
14.0	-.005	-.004	-.005	.005	-.005	-.008	-.006	.002	-.010	-.013	-.010	-.004	-.017	-.015	-.014	-.012	-.018	-.018	-.016	-.014
45.0	-.010	-.010	-.010	-.012	-.011	-.011	-.012	-.012	-.013	-.012	-.013	-.013	-.013	-.013	-.014	-.014	-.013	-.011	-.014	-.014

TABLE III - EXTERNAL AND INTERNAL PRESSURE COEFFICIENTS OF NACA 8-INCH RAM-JET CONFIGURATION FOR FOUR ANGLES OF ATTACK AT FREE-STREAM MACH NUMBER OF 1.79 - Continued

Station	$\alpha = 3^\circ$; $m_3/m_0 = 0.939$				$\alpha = 3^\circ$; $m_3/m_0 = 0.893$				$\alpha = 3^\circ$; $m_3/m_0 = 0.762$				$\alpha = 3^\circ$; $m_3/m_0 = 0.586$				$\alpha = 3^\circ$; $m_3/m_0 = 0.303$			
	(a) Continued. Longitudinal distribution of C_p.																			
	Outer shell			Center body	Outer shell			Center body	Outer shell			Center body	Outer shell			Center body	Outer shell			Center body
	External		Internal		External		Internal		External		Internal		External		Internal		External		Internal	
θ→	180°	270°	0°	0°	180°	270°	0°	0°	180°	270°	0°	0°	180°	270°	0°	0°	180°	270°	0°	0°
-1.0				0.578				0.579				0.675				1.278				1.373
-0.5				.577				.586				1.222				1.326				1.429
0				.577				1.140				1.231				1.377				1.492
0.5	0.098	0.214	0.964	0.477	0.019	0.137	1.163	.842	-0.099	0.004	1.331	1.071	-0.263	-0.194	1.512	1.339	-0.332	-0.329	1.613	1.522
1.0	.080	.159	.975	.953	.048	.126	1.145	1.075	-.033	.057	1.311	1.246	-.159	-.070	1.491	1.453	-.323	-.263	1.598	1.573
1.5	.057	.125	1.019	.985	.036	.104	1.168	1.142	-.013	.064	1.322	1.298	-.107	-.029	1.494	1.482	-.257	-.136	1.596	1.588
2.0		.097	1.019	1.004		.081	1.176	1.163		.061	1.326	1.316		-.016	1.495	1.494		-.100	1.596	1.594
2.5	.082	.084	1.019	1.010	.032	.072	1.178	1.173	.010	.049	1.331	1.325	-.062	-.003	1.497	1.499	-.124	-.059	1.596	1.596
3.0		.067	1.024	1.013		.056	1.186	1.178		.037	1.334	1.329		0.003	1.500	1.500		-.056	1.598	1.596
4.0	-.001	.040	1.026	1.027	-.010	.037	1.191	1.194	-.028	.023	1.340	1.342	-.057	-.003	1.503	1.509	-.095	-.040	1.599	1.599
5.0	-.006	.027	.998	.996	-.013	.023	1.186	1.165	-.028	.010	1.340	1.340	-.051	-.012	1.505	1.509	-.077	-.036	1.601	1.599
6.0	-.015	.008	.963	.936	-.023	.004	1.179	1.160	-.033	-.006	1.340	1.325	-.052	-.023	1.507	1.503	-.072	-.043	1.601	1.599
7.0		-.004	.897	.896		-.008	1.158	1.153		-.016	1.329	1.325		-.030	1.503	1.503		-.045	1.599	1.599
8.0	-.021	-.007	.922	.893	-.026	-.009	1.176	1.153	-.033	-.018	1.359	1.323	-.045	-.030	1.509	1.503	-.059	-.043	1.602	1.599
9.0	-.024	-.015	.860	.897	-.026	-.016	1.161	1.155	-.031	-.024	1.332	1.345	-.041	-.034	1.507	1.514	-.053	-.046	1.602	1.604
10.0	-.027	-.021		.801	-.029	-.022		1.188	-.037	-.027		1.349	-.045	-.037		1.517	-.053	-.046		1.604
11.0	-.020	-.018		.603	-.021	-.020		1.206	-.028	-.026		1.360	-.036	-.034		1.521	-.043	-.044		1.604
12.0	-.015	-.015		.456	-.016	-.013		1.241	-.022	-.019		1.381	-.030	-.026		1.528	-.036	-.036		1.607
14.0	-.007	-.008		.289	-.011	-.009		1.311	-.012	-.015		1.424	-.018	-.022		1.544	-.022	-.028		1.612
16.0	-.009	0		.636	-.011	-.009		1.368	-.013	-.013		1.469	-.018	-.019		1.559	-.022	-.025		1.616
18.0	.001	-.004		.865	0	-.008		1.406	-.003	-.012		1.487	-.007	-.016		1.572	-.012	-.022		1.620
21.0	.005	-.005		1.064	.004	-.008		1.463	.003	-.011		1.526	-.002	-.015		1.591	-.006	-.020		1.625
24.0	.009	-.003		1.183	.008	-.004		1.513	.005	-.005		1.556	.003	-.008		1.607	-.001	-.012		1.632
27.0	.002	.001		1.375	-.003	.001		1.554	0	-.003		1.582	-.003	-.005		1.619	-.006	-.008		1.636
31.0	.004			1.332	.004			1.580	.003			1.595	.002			1.626	-.002			1.639
35.0	-.020				-.019				-.021				-.022				-.025			
37.0				1.373				1.621				1.624				1.636				1.640
40.0	-.010				-.009				-.011				-.011				-.012			
45.0	-.012				-.012				-.012				-.013				-.015			

(b) Continued. Circumferential distribution of C_p.

Station	Outer shell, external				Outer shell, external				Outer shell, external				Outer shell, external				Outer shell, external			
θ→	198°	216°	234°	252°	198°	216°	234°	252°	198°	216°	234°	252°	198°	216°	234°	252°	198°	216°	234°	252°
0.5	0.120	0.143	0.163	0.186	0.036	0.063	0.084	0.107	-0.081	-0.060	-0.059	-0.023	-0.255	-0.240	-0.227	-0.221	-0.332	-0.332	-0.330	-0.332
14.0	-.015	-.015	-.010	-.002	-.016	-.013	-.013	-.007	-.019	-.022	-.018	-.011	-.026	-.028	-.023	-.016	-.029	-.033	-.030	-.023
43.0	-.013	-.013	-.017	-.020	-.013	-.013	-.018	-.021	-.013	-.013	-.018	-.021	-.016	-.015	-.018	-.022	-.017	-.017	-.020	-.023

[redacted]

TABLE III - EXTERNAL AND INTERNAL PRESSURE COEFFICIENTS OF NACA 8-INCH RAM-JET CONFIGURATION FOR FOUR ANGLES OF ATTACK AT FREE-STREAM MACH NUMBER OF 1.79 - Continued

Station	$\alpha = 6^\circ$; $m_3/m_0 = 0.935$				$\alpha = 6^\circ$; $m_3/m_0 = 0.898$				$\alpha = 6^\circ$; $m_3/m_0 = 0.720$				$\alpha = 6^\circ$; $m_3/m_0 = 0.644$			
	(a) Continued. Longitudinal distribution of C_p.															
	Outer shell			Center body	Outer shell			Center body	Outer shell			Center body	Outer shell			Center body
	External		Internal		External		Internal		External		Internal		External		Internal	
$\theta \rightarrow$	180°	270°	0°	0°	180°	270°	0°	0°	180°	270°	0°	0°	180°	270°	0°	0°
-1.0				0.663				0.663				0.791				1.225
-0.5				.660				.660				1.228				1.272
0				.682				1.037				1.243				1.295
0.5	-0.009	0.229	0.784	.326	-0.077	0.157	1.051	.691	-0.222	-0.012	1.315	1.085	-0.297	-0.090	1.390	1.185
1.0	.003	.170	.561	.386	-.038	.141	1.065	1.014	-.139	.048	1.311	1.257	-.192	-.005	1.382	1.333
1.5	-.012	.134	.967	.960	-.038	.116	1.130	1.096	-.106	-.039	1.334	1.313	-.147	.026	1.396	1.380
2.0		.105	1.001	1.002		.092	1.142	1.134		.049	1.344	1.338		.025	1.407	1.400
2.5	-.017	.090	1.006	.999	-.017	.083	1.154	1.152	-.080	.049	1.353	1.350	-.106	.030	1.413	1.410
3.0		.072	1.014	1.002		.065	1.166	1.162		.037	1.361	1.358		.022	1.419	1.416
4.0	-.044	.039	1.017	1.019	-.063	.036	1.176	1.185	-.078	.020	1.370	1.376	-.092	.008	1.429	1.431
5.0	-.041	.021	.993	.990	-.049	.019	1.178	1.180	-.070	.003	1.376	1.378	-.080	-.005	1.433	1.433
6.0	-.044	.001	.958	.933	-.051	-.002	1.176	1.160	-.067	-.016	1.377	1.367	-.074	-.021	1.436	1.428
7.0		-.015	.896	.894		-.018	1.158	1.155		-.029	1.369	1.367		-.035	1.430	1.429
8.0	-.037	-.022	.911	.883	-.041	-.023	1.177	1.158	-.052	-.034	1.377	1.365	-.056	-.039	1.437	1.428
9.0	-.037	-.033	.845	.881	-.038	-.034	1.165	1.191	-.046	-.044	1.370	1.384	-.050	-.049	1.453	1.442
10.0	-.038	-.041		.781	-.043	-.041		1.195	-.050	-.049		1.388	-.052	-.052		1.445
11.0	-.028	-.036		.583	-.030	-.041		1.211	-.036	-.049		1.396	-.039	-.054		1.454
12.0	-.018	-.033		.421	-.020	-.040		1.244	-.027	-.047		1.413	-.027	-.082		1.467
14.0	-.014	-.034		.275	-.015	-.040		1.309	-.021	-.047		1.446	-.021	-.060		1.492
16.0	-.007	-.033		.686	-.009	-.036		1.362	-.013	-.044		1.476	-.013	-.047		1.514
18.0	-.003	-.034		.887	-.001	-.036		1.403	-.004	-.042		1.500	-.005	-.044		1.533
21.0	.006	-.034		1.057	.005	-.036		1.454	-.002	-.041		1.534	0	-.042		1.560
24.0	.009	-.028		1.180	.008	-.031		1.500	.003	-.035		1.563	.003	-.036		1.583
27.0	.003	-.025		1.268	.003	-.028		1.541	-.002	-.029		1.585	-.002	-.031		1.602
31.0	.005			1.324	.004			1.568	.002			1.595	.002			1.610
35.0	-.020				-.022				-.023				-.024			
37.0				1.365				1.611				1.620				1.628
40.0	-.008				-.008				.011				-.011			
45.0	-.011				-.011				-.013				-.013			

(b) Continued. Circumferential distribution of C_p.

Station	Outer shell, external				Outer shell, external				Outer shell, external				Outer shell, external			
$\theta \rightarrow$	198°	216°	234°	252°	198°	216°	234°	252°	198°	216°	234°	252°	198°	216°	234°	252°
0.5	0.019	0.062	0.107	0.161	-0.052	-0.014	0.040	0.083	-0.193	-0.154	-0.114	-0.074	-0.284	-0.246	-0.192	-0.154
14.0	-.018	-.028	-.035	-.032	-.020	-.030		-.037	-.026	-.036	-.044	-.046	-.027	-.038	-.046	-.049
43.0	-.017	-.020	-.028	-.038	-.017	-.020	-.028	-.040	-.019	-.023	-.028	-.041	-.019	-.023	-.028	-.041

[redacted]

TABLE III - EXTERNAL AND INTERNAL PRESSURE COEFFICIENTS OF NACA 8-INCH RAM-JET CONFIGURATION FOR FOUR ANGLES OF ATTACK AT FREE-STREAM-MACH NUMBER OF 1.79 - Concluded

Station	$\alpha = 6^\circ$; $m_3/m_0 = 0.302$				$\alpha = 10^\circ$; $m_3/m_0 = 0.916$				$\alpha = 10^\circ$; $m_3/m_0 = 0.893$				$\alpha = 10^\circ$; $m_3/m_0 = 0.722$			
	(a) Concluded. Longitudinal distribution of C_p.															
	Outer shell			Center body	Outer shell			Center body	Outer shell			Center body	Outer shell			Center body
	External		Internal		External		Internal		External		Internal		External		Internal	
$\theta \rightarrow$	180°	270°	0°	0°	180°	270°	0°	0°	180°	270°	0°	0°	180°	270°	0°	0°
-1.0				1.387				0.777				0.777				0.947
-0.5				1.452				.799				.798				1.167
0				1.485				.795				.830				1.190
0.5	-0.342	-0.318	1.596	1.515	-0.135	0.241	0.677	.539	-0.204	0.181	1.227	.568	-0.260	0.026	1.196	.986
1.0	-.329	-.189	1.585	1.562	-.102	.184	.516	.267	-.174	.171	.986	.936	-.214	.085	1.228	1.182
1.5	-.306	-.113	1.586	1.580	-.103	.146	.362	.148	-.136	.141	1.067	1.052	-.189	.088	1.273	1.253
2.0		-.080	1.588	1.586		.113	.664	.409		.109	1.106	1.095		.075	1.292	1.288
2.5	-.174	-.052	1.590	1.589	-.091	.095	.850	.880	-.102	.093	1.129	1.124	-.149	.065	1.309	1.310
3.0		-.043	1.593	1.591		.072	.950	.945		.070	1.151	1.143		.047	1.325	1.324
4.0	-.142	-.028	1.596	1.596	-.094	.031	.979	.976	-.110	.034	1.172	1.175	-.136	.021	1.341	1.349
5.0	-.116	-.034	1.598	1.596	-.074	.010	.962	.958	-.091	.010	1.180	1.177	-.114	-.004	1.353	1.354
6.0	-.103	-.044	1.600	1.596	-.064	-.016	.930	.906	-.074	-.019	1.183	1.164	-.093	-.029	1.358	1.349
7.0		-.052	1.598	1.598		-.036	.875	.871		-.038	1.177	1.169		-.048	1.353	1.353
8.0	-.070	-.054	1.601	1.600	-.045	-.048	.875	.848	-.051	-.048	1.199	1.179	-.057	-.057	1.364	1.353
9.0	-.069	-.062	1.601	1.605	-.044	-.064	.799	.832	-.046	-.065	1.205	1.218	-.060	-.072	1.356	1.373
10.0	-.058	-.065		1.604	-.040	-.069		.723	-.043	-.074		1.229	-.048	-.081		1.377
11.0	-.043			1.604	-.025	-.078		.526	-.030	-.079		1.245	-.034	-.086		1.387
12.0	-.031	-.064		1.606	-.020	-.080		.372	-.025	-.088		1.273	-.027	-.095		1.403
14.0	-.026	-.060		1.611	-.009	-.086		.234	-.014	-.096		1.327	-.017	-.101		1.438
16.0	-.016	-.057		1.616	-.004	-.096		.778	-.006	-.104		1.371	-.008	-.111		1.470
18.0	-.007	-.050		1.619	.006	-.102		.924	.004	-.112		1.406	.001	-.118		1.495
21.0	-.003	-.046		1.624	.011	-.107		1.058	.008	-.117		1.453	.005	-.124		1.528
24.0	0	-.037		1.629	.014	-.097		1.161	.012	-.108		1.495	.009	-.111		1.559
27.0	-.004	-.030		1.632	.011	-.085		1.230	.008	-.094		1.533	.006	-.095		1.562
31.0	0			1.635	.012			1.272	.011			1.561	.009			1.595
35.0	-.026				-.020				-.023				-.026			
37.0				1.637				1.518				1.600				1.617
40.0	-.011				-.005				-.004				-.006			
45.0	-.013				-.012				-.012				-.012			
	(b) Concluded. Circumferential distribution of C_p.															
Station	Outer shell, external				Outer shell, external				Outer shell, external				Outer shell, external			
$\theta \rightarrow$	198°	216°	234°	252°	198°	216°	234°	252°	198°	216°	234°	252°	198°	216°	234°	252°
0.5	-0.342	-0.337	-0.329	-0.325	-0.104	-0.045	0.037	0.139	-0.176	-0.125	-0.061	-0.048	-0.251	-0.209	-0.157	-0.084
14.0	-.051	-.042	-.052	-.058	-.022	-.045	-.078	-.104	-.026	-.050	-.086	-.117	-.029	-.053	-.090	-.124
45.0	-.019	-.025	-.028	-.041	-.033	-.042	-.045	-.062	-.033	-.045	-.046	-.064	-.033	-.045	-.047	-.064

[redacted]

[redacted]

TABLE IV - EXTERNAL AND INTERNAL PRESSURE COEFFICIENTS OF NACA 8-INCH RAM-JET CONFIGURATION FOR FOUR ANGLES OF ATTACK AT FREE-STREAM MACH NUMBER OF 1.79 WITH MODEL ROTATED 180°

(a) Longitudinal distribution of C_p.

Station	$\alpha = 0^\circ$; $m_3/m_0 = 0.840$				$\alpha = 0^\circ$; $m_3/m_0 = 0.885$				$\alpha = 0^\circ$; $m_3/m_0 = 0.754$				$\alpha = 0^\circ$; $m_3/m_0 = 0.519$			
	Outer shell			Center body	Outer shell			Center body	Outer shell			Center body	Outer shell			Center body
	External		Internal		External		Internal		External		Internal		External		Internal	
$\theta \rightarrow$	0°	90°	180°	180°	0°	90°	180°	180°	0°	90°	180°	180°	0°	90°	180°	180°
-1.0				0.503				0.504				0.605				1.276
-0.5				.504				.583				1.234				1.333
0				.522				1.187				1.258				1.397
0.5	0.215	0.217		.898	0.116	0.118		.970	-0.006	-0.008		1.134	-0.243	-0.260		1.374
1.0	.162	.163	1.066	.999	.118	.121	1.219	1.153	.052	.057	1.344	1.291	-.069	-.056	1.516	1.480
1.5	.118	.129			.090	.101			.050	.061			-.046	-.037		
2.0	.095	.100	1.066	1.036	.073	.079	1.228	1.203	.044	.051	1.357	1.339	-.028	-.022	1.517	1.508
2.5	.081	.088		1.048	.064	.071		1.219	.043	.049		1.351	-.012	-.004		1.517
3.0		.071		1.046		.058		1.219		.038		1.352		-.004		1.518
4.0	.037	.045	1.054	1.055	.028	.037	1.224	1.227	.012	.021	1.352	1.358	-.017	-.007	1.517	1.520
5.0	.025	.031		1.023	.020	.025		1.216	.005	.012		1.352	-.017	-.010		1.520
6.0	.013	.015	.987	.959	.006	.009	1.205	1.185	-.004	-.002	1.348	1.335	-.022	-.018	1.517	1.511
7.0		.003		.919		-.001		1.175		-.010		1.331		-.023		1.510
8.0	.004	.004		.912	-.001	.002		1.167	-.010	-.007		1.324	-.022	-.018		1.506
9.0		0		.922		.004		1.187		-.004		1.344		-.012		1.516
10.0	.001	0		.847	.004	.002		1.180	.003	-.005		1.344	-.012	-.013		1.516
11.0	.003	-.003		.909	.001	-.004		1.198	-.008	-.011		1.365	-.015	-.018		1.521
12.0	.004	.008		1.010	.004	.012		1.237	-.008	.007		1.376	.010	.001		1.528
14.0	-.004	.007		1.069	-.006	.004		1.309	-.010	0		1.419	-.015	-.005		1.546
16.0	-.012	-.005		1.244	-.014	-.010		1.367	-.020	-.015		1.456	-.025	-.020		1.560
18.0	.014	-.007		1.315	.007	-.009		1.412	.003	-.012		1.486	0	-.013		1.573
21.0	.017	.007		1.405	.012	.002		1.474	.006	.003		1.525	.004	-.006		1.592
24.0	.014	.001		1.484	.009	-.002		1.525	.006	.005		1.558	.003	-.007		1.609
27.0	.004	.005		1.536	.009	.002		1.565	-.002	0		1.586	-.004	-.002		1.622
31.0	.004			1.574	.002			1.591	0			1.599	-.002			1.627
35.0	-.020				-.019				-.020				-.021			
37.0				1.615				1.627				1.626				1.637
40.0	-.007				.007				-.010				-.008			
45.0	-.011				-.010				-.012				-.012			

(b) Circumferential distribution of C_p.

Station	Outer shell, external				Outer shell, external				Outer shell, external				Outer shell, external			
$\theta \rightarrow$	18°	36°	54°	72°	18°	36°	54°	72°	18°	36°	54°	72°	18°	36°	54°	72°
0.5	0.226	0.234	0.235	0.226	0.124	0.133	0.134	0.124	0	0.008	0.012	0.001	-0.240	-0.227	-0.217	-0.244
14.0	-.004	-.007	-.006	.005	-.009	-.013	-.011	.006	-.015	-.020	-.014	0	-.021	-.025	-.021	-.006
43.0	-.008	-.008	-.010	-.012	-.010	-.009	-.012	-.012	-.011	-.011	-.012	-.013	-.011	-.010	-.012	-.013

[redacted]

TABLE IV - EXTERNAL AND INTERNAL PRESSURE COEFFICIENTS [illegible]A 8-INCH RAM-JET CONFIGURATION
FOR FOUR ANGLES OF ATTACK AT FREE-STREAM MACH NUMBER OF [illegible]ITH MODEL ROTATED 180° - Continued

Station	α = 0°; m_3/m_0 = 0.885				α = 3°; m_3/m_0 = 0.940				α = 3°; m_3/m_0 = 0.893				α = 3°; m_3/m_0 = 0.754			
	(a) Continued. Longitudinal distribution of C_p.															
	Outer shell			Center body	Outer shell			Center body	Outer shell			Center body	Outer shell			Center body
	External		Internal		External		Internal		External		Internal		External		Internal	
θ →	0°	90°	180°	180°	0°	90°	180°	180°	0°	90°	180°	180°	0°	90°	180°	180°
-1.0				1.369				0.432				0.432				0.526
-0.5				1.434				.431				.506				1.168
0				1.503				.527				1.152				1.252
0.5	-0.333	-0.333		1.538	0.325	0.201		960	0.277	-0.138		1.031	0.139	0.010		1.178
1.0	-.248	-.248	1.606	1.597	.252	.158	1.163	1.087	.230	.131	1.238	1.177	.167	.060	1.365	1.313
1.5	-.140	-.129			.197	.124			.181	.107			.147	.069		
2.0	-.099	-.094	1.605	1.602	.165	.098	1.131	1.101	.152	.083	1.231	1.208	.128	.056	1.370	1.352
2.5	-.071	-.064		1.605	.146	.084		1.107	.135	.073		1.215	.116	.054		1.358
3.0		-.051		1.605		.068		1.097		.059		1.210		.041		1.355
4.0	-.048	-.038	1.605	1.606	.087	.042	1.100	1.099	.080	.038	1.205	1.210	.066	.024	1.353	1.356
5.0	-.039	-.030		1.605	.072	.027		1.071	.064	.025		1.191	.053	.013		1.345
6.0	-.039	-.035	1.603	1.602	.051	.010	1.043	1.017	.046	.008	1.172	1.152	.034	-.002	1.337	1.323
7.0		-.036		1.602		-.001		.982		-.004		1.131		-.012		1.312
8.0	-.033	-.028		1.602	.033	-.003		.966	.031	-.003		1.108	.021	-.010		1.298
9.0		-.023		1.602		-.007		.961		0		1.111		-.007		1.309
10.0	-.023	-.023		1.602	.038	-.007		.880	.033	-.005		1.086	.022	-.012		1.306
11.0	-.025	-.025		1.603	.021	-.010		.933	.018	-.010		1.106	.009	-.015		1.313
12.0	-.018	-.007		1.604	.059	.005		1.032	.036	.003		1.156	.026	-.003		1.337
14.0	-.022	-.012		1.610	.023	.005		1.170	.020	-.001		1.250	.012	-.007		1.388
16.0	-.030	-.024		1.615	.008	-.015		1.263	.006	-.018		1.323	.001	-.022		1.431
18.0	-.005	-.016		1.619	.008	-.018		1.334	.006	-.018		1.379	.004	-.019		1.466
21.0	0	-.010		1.626	.023	-.005		1.426	.021	-.007		1.455	.015	-.010		1.513
24.0	-.002	-.010		1.630	.021	-.010		1.502	.020	-.010		1.516	.015	-.012		1.553
27.0	-.007	-.004		1.635	.008	-.007		1.551	.006	-.008		1.558	.004	-.009		1.583
31.0	-.003			1.638	.010			1.586	.008			1.583	.006			1.598
35.0	-.023				-.016				-.018				-.018			
37.0				1.639				1.638				1.619				1.624
40.0	-.010				-.005				-.005				-.006			
45.0	-.013				-.010				-.010				-.010			

(b) Continued. Circumferential distribution of C_p.

Station	Outer shell, external				Outer shell, external				Outer shell, external				Outer shell, external			
θ →	18°	36°	54°	72°	18°	36°	54°	72°	18°	36°	54°	72°	18°	36°	54°	72°
0.5	-0.334	-0.334	-0.332	-0.334	0.329	0.321	0.296	0.252	0.278	0.269	0.240	0.189	0.141	0.132	0.109	0.054
14.0	-.027	-.030	-.025	-.012	-.016	.008	.003	.018	.013	.005	.001	.010	.007	-.002	-.007	-.004
45.0	-.012	-.012	-.013	-.015	-.007	-.010	-.015	-.020	-.008	-.010	-.015	-.020	-.009	-.011	-.015	-.020

[redacted]

CONFIDENTIAL

TABLE IV - EXTERNAL AND INTERNAL PRESSURE COEFFICIENTS OF NACA 8-INCH RAM-JET CONFIGURATION FOR FOUR ANGLES OF ATTACK AT FREE-STREAM MACH NUMBER OF 1.79 WITH MODEL ROTATED 180° - Continued

NACA

(a) Continued. Longitudinal distribution of C_p.

Station	$\alpha = 3^\circ$; $m_3/m_0 = 0.517$				$\alpha = 3^\circ$; $m_3/m_0 = 0.291$				$\alpha = 6^\circ$; $m_3/m_0 = 0.940$				$\alpha = 6^\circ$; $m_3/m_0 = 0.886$			
	Outer shell			Center body	Outer shell			Center body	Outer shell			Center body	Outer shell			Center body
	External		Internal		External		Internal		External		Internal		External		Internal	
θ →	0°	90°	180°	180°	0°	90°	180°	180°	0°	90°	180°	180°	0°	90°	180°	180°
-1.0				1.263				1.353				0.364				0.363
-0.5				1.329				1.427				.363				.429
0				1.401				1.505				.448				1.160
0.5	-0.086	-0.230		1.391	-0.307	-0.336		1.545	0.448	0.226		1.026	0.420	0.131		1.120
1.0	.023	-.083	1.525	1.491	-.123	-.251	1.616	1.595	.345	.174	1.195	1.117	.329	.132	1.307	1.238
1.5	.049	-.032			-.055	-.132			.278	.159			.267	.111		
2.0	.059	-.018	1.525	1.517	-.018	-.094	1.611	1.608	.237	.108	1.124	1.090	.229	.088	1.277	1.254
2.5	.064	-.003		1.523	.004	-.064		1.608	.214	.094		1.092	.209	.080		1.264
3.0		-.003		1.522		-.052		1.608		.076		1.076		.063		1.242
4.0	.038	-.007	1.517	1.522	.009	-.038	1.606	1.608	.140	.046	1.068	1.069	.156	.034	1.232	1.234
5.0	.031	-.010		1.517	.009	-.032		1.601	.118	.027		1.028	.114	.018		1.210
6.0	.016	-.020	1.512	1.507		-.038	1.603	1.601	.094	.007	.988	.960	.090	0	1.187	1.167
7.0		-.026		1.503		-.040		1.599		-.008		.908		-.015		1.137
8.0	.008	-.023		1.497	-.004	-.033		1.596	.068	-.013		.914	.083	-.017		1.097
9.0		-.018		1.502		-.030		1.598		-.020		.926		-.019		1.073
10.0	.010	-.021		1.500	0	-.031		1.596	.071	-.021		.824	.067	-.024		1.017
11.0	-.003	-.024		1.504	-.010	-.031		1.598	.061	-.018		.629	.047	-.027		1.038
12.0	.008	-.010		1.513	.009	-.018		1.601	.080	-.015		.457	.059	-.025		1.104
14.0	.005	-.015		1.533	-.002	-.020		1.607	.059	-.020		1.049	.055	-.030		1.217
16.0	-.007	-.028		1.551	-.012	-.033		1.613	.038	-.040		1.175	.022	-.047		1.300
18.0	0	-.023		1.567	-.003	-.024		1.618	.026	-.046		1.263	.024	-.048		1.365
21.0	.010	-.013		1.588	.006	-.018		1.624	.041	-.030		1.374	.037	-.035		1.447
24.0	.010	-.015		1.607	.006	-.018		1.631	.038	-.033		1.462	.035	-.038		1.512
27.0	.001	-.010		1.621	-.002	-.013		1.635	.025	-.033		1.517	.022	-.037		1.552
31.0	.004			1.628	.002			1.638	.024			1.558	.020			1.577
35.0	-.018				-.026				-.003				-.005			
37.0				-1.636				1.641				1.594				1.615
40.0	-.007				-.008				.005				.004			
45.0	-.010				-.012				.002				-.002			

(b) Continued. Circumferential distribution of C_p.

Station	Outer shell, external				Outer shell, external				Outer shell, external				Outer shell, external			
θ →	18°	36°	54°	72°	18°	36°	54°	72°	18°	36°	54°	72°	18°	36°	54°	72°
0.5	-0.086	-0.091	-0.114	-0.168	-0.311	-0.312	-0.315	-0.332	0.445	0.424	0.379	0.310	0.418	0.389	0.324	0.230
14.0	-.002	-.010	-.015	-.005	-.007	-.017	-.020	-.010	.049	.028	.009	.003	.044	.024	.003	
43.0	-.010	-.012	-.016	-.021	-.010	-.012	-.018	-.021	.002	-.010	-.024	-.040	-.002	-.012	-.028	-.043

CONFIDENTIAL

TABLE IV - EXTERNAL AND INTERNAL PRESSURE COEFFICIENTS OF NACA 8-INCH RAM-JET CONFIGURATION FOR FOUR ANGLES OF ATTACK AT FREE-STREAM MACH NUMBER OF 1.79 WITH MODEL ROTATED 180° - Concluded

Station	$\alpha = 6°$; $m_3/m_0 = 0.762$				$\alpha = 6°$; $m_3/m_0 = 0.518$				$\alpha = 10°$; $m_3/m_0 = 0.930$				$\alpha = 10°$; $m_3/m_0 = 0.885$			
	(a) Concluded. Longitudinal distribution of C_p.															
	Outer shell			Center body	Outer shell			Center body	Outer shell			Center body	Outer shell			Center body
	External		Internal		External		Internal		External		Internal		External		Internal	
$\theta \rightarrow$	0°	90°	180°	180°	0°	90°	180°	180°	0°	90°	180°	180°	0°	90°	180°	180°
-1.0				0.435				1.245				0.308				0.764
-0.5				1.128				1.324				.308				.768
0				1.280				1.406				.739				.813
0.5	0.300	0.008		1.221	0.049	-0.189		1.406	0.591	0.244		.930	0.593	0.168		.929
1.0	.284	.071	1.407	1.341	.140	-.070	1.536	1.506	.450	.195	1.164	1.083	.455	.182	1.201	1.114
1.5	.241	.077			.150	-.025			.368	.156			.375	.149		
2.0	.212	.059	1.388	1.370	.145	-.012	1.534	1.529	.318	.120	1.107	1.093	.324	.110	1.252	1.294
2.5	.194	.058		1.372	.141	.004		1.531	.288	.101		1.078	.294	.097		1.286
3.0		.044		1.365		.001		1.528		.080		1.058		.074		1.266
4.0	.127	.021	1.357	1.360	.095	-.005	1.620	1.525	.205	.047	1.048	1.048	.212	.043	1.220	1.233
5.0	.106	.008		1.344	.079	-.014		1.517	.178	.026		1.013	.186	.021		1.198
6.0	.063	-.010	1.329	1.314	.060	-.025	1.509	1.504	.148	.001	.978	.951	.155	-.007	1.161	1.146
7.0		-.022		1.296		-.057		1.496		-.023		.906		-.030		1.104
8.0	.058	-.023		1.267	.041	-.037		1.486	.118	-.036		.904	.124	-.041		1.059
9.0		-.025		1.267		-.035		1.489		-.048		.906		-.053		1.016
10.0	.059	-.030		1.249	.044	-.037		1.484	.112	-.061		.797	.117	-.066		.959
11.0	.041	-.032		1.260	.026	-.044		1.487	.094	-.074		.601	.098	-.078		.964
12.0	.052	-.031		1.287	.041	-.043		1.494	.102	-.081		.429	.106	-.083		1.039
14.0	.049	-.034		1.352	.026	-.043		1.519	.100	-.085		.956	.101	-.083		1.166
16.0	.051	-.061		1.408	.021	-.057		1.539	.081	-.096		1.100	.083	-.099		1.256
18.0	.019	-.048		1.445	.010	-.048		1.557	.069	-.105		1.195	.074	-.102		1.323
21.0	.056	-.037		1.503	.026	-.040		1.581	.076	-.101		1.309	.076	-.103		1.412
24.0	.032	-.038		1.548	.024	-.040		1.601	.070	-.104		1.395	.072	-.105		1.480
27.0	.021	-.038		1.578	.014	-.037		1.618	.067	-.101		1.446	.060	-.100		1.522
31.0	.020			1.591	.016			1.621	.053			1.481	.067			1.549
35.0	-.007				-.010				.022				.028			
37.0				1.618				1.632				1.513				1.584
40.0	.003				.001				.030				.035			
45.0	-.002				-.003				.023				.029			

(b) Concluded. Circumferential distribution of C_p.																
Station	Outer shell, external				Outer shell, external				Outer shell, external				Outer shell, external			
$\theta \rightarrow$	18°	36°	54°	72°	18°	36°	54°	72°	18°	36°	54°	72°	18°	36°	54°	72°
0.5	0.292	0.257	0.194	0.102	0.034	0.009	-0.037	-0.113	0.586	0.541	0.468	0.368	0.590	0.548	0.472	0.346
14.0	.038	.019	-.001	-.010	.027	.009	-.010	-.021	.086	.056	.007	-.035	.086	.053	.004	-.040
43.0	-.002	-.012	-.027	-.043	-.003	-.014	-.028	-.043	.018	-.014	-.052	-.089	.022	-.010	-.049	-.087

TABLE V - EXTERNAL AND INTERNAL PRESSURE COEFFICIENTS OF NACA 8-INCH RAM-JET CONFIGURATION FOR FOUR ANGLES OF ATTACK AT FREE-STREAM MACH NUMBER OF 1.99

(a) Longitudinal distribution of C_p.

Station	$\alpha = 0^\circ$; $m_3/m_0 = 1.00$				$\alpha = 0^\circ$; $m_3/m_0 = 0.901$				$\alpha = 0^\circ$; $m_3/m_0 = 0.732$				$\alpha = 0^\circ$; $m_3/m_0 = 0.445$				$\alpha = 0^\circ$; $m_3/m_0 = 0.287$			
	Outer shell			Center body	Outer shell			Center body	Outer shell			Center body	Outer shell			Center body	Outer shell			Center body
	External		Internal		External		Internal		External		Internal		External		Internal		External		Internal	
θ →	180°	270°	0°	0°	180°	270°	0°	0°	180°	270°	0°	0°	180°	270°	0°	0°	180°	270°	0°	0°
-1.0				0.477				0.475				0.587				1.401				1.423
-0.5				.477				.492				1.240				1.441				1.492
0				.477				1.125				1.400				1.504				1.562
0.5	0.210	0.204	0.539	.215	0.157	0.157	1.308	1.075	0.005	0.003	1.498	1.238	-0.200	-0.206	1.636	1.476	0.243	-0.244	1.675	1.576
1.0	.157	.151	.707	.143	.135	.130	1.291	1.247	.064	.060	1.473	1.411	-.072	-.075	1.616	1.589	-.154	-.161	1.662	1.545
1.5	.123	.121	.503	.402	.106	.104	1.268	1.300	.066	.063	1.473	1.454	-.028	-.026	1.514	1.610	-.075	-.074	1.659	1.659
2.0	.101	.098	.306	.606	.087	.081	1.277	1.316	.059	.052	1.473	1.468	-.004	-.014	1.615	1.620	-.040	-.050	1.660	1.664
2.5	.089	.086	.456	.554	.077	.071	1.286	1.319	.052	.049	1.473	1.473	.005	0	1.615	1.621	-.026	-.028	1.660	1.665
3.0	.072	.070	.582	.392	.061	.057	1.301	1.318	.037	.038	1.475	1.473	.001	0	1.617	1.621	-.022	-.022	1.662	1.664
4.0	.047	.047	.415	.692	.037	.041	1.295	1.331	.022	.024	1.476	1.483	-.005	0	1.620	1.626	-.018	-.015	1.663	1.667
5.0	.036	.033	.551	.436	.027	.025	1.308	1.320	.012	.012	1.475	1.478	-.005	-.000	1.622	1.626	-.016	-.018	1.664	1.667
6.0	.022	.018	.491	.540	.014	.012	1.302	1.297	.001	0	1.473	1.465	-.016	-.017	1.624	1.622	-.022	-.023	1.665	1.665
7.0	.007	.007	.537	.465	-.002	.002	1.288	1.290	-.013	-.009	1.466	1.465	-.027	-.023	1.622	1.622	-.032	-.028	1.664	1.664
8.0	.007	.005	.596	.399	0	.001	1.295	1.279	-.010	-.009	1.473	1.456	-.022	-.022	1.624	1.621	-.027	-.027	1.665	1.664
9.0	0	-.005	.445	.494	-.004	-.008	1.276	1.303	-.012	-.017	1.466	1.476	-.023	-.028	1.622	1.627	-.027	-.032	1.665	1.668
10.0	-.012	-.010		.790	-.021	-.010		1.301	-.029	-.019		1.480	-.038	-.029		1.629	-.042	-.033		1.669
11.0	0	-.008		.579	-.007	-.012		1.315	-.014	-.019		1.488	-.024	-.029		1.632	-.027	-.032		1.669
12.0	.005	-.003		.476	-.002	-.005		1.346	-.010	-.012		1.505	-.019	-.021		1.637	-.023	-.024		1.672
14.0	.005	-.001		.997	0	-.002		1.410	-.008	-.009		1.541	-.014	-.016		1.650	-.018	-.018		1.677
16.0	.005	.004		1.129	0	-.002		1.463	-.007	-.008		1.579	-.013	-.016		1.661	-.015	-.018		1.683
18.0	.010	.004		1.224	.006	.001		1.508	.001	-.005		1.598	-.005	-.012		1.672	-.008	-.013		1.687
21.0	.015	.005		1.341	.011	.003		1.566	.006	-.002		1.636	.001	-.007		1.687	-.008	-.009		1.694
24.0	.026	.017		1.435	.020	.014		1.620	.014	.010		1.673	.008	.005		1.701	.006	.002		1.701
27.0	-.002	.007		1.504	-.007	.003		1.661	-.010	0		1.700	-.016	-.005		1.709	-.017	-.007		1.706
31.0	0			1.550	.001			1.683	0			1.714	-.002			1.716	-.004			1.707
35.0	-.017				-.019				-.021								-.024			
37.0				1.598				1.718				1.731				1.720				1.709
40.0	-.010				-.012				-.012				-.014				-.016			
45.0	-.006				-.008				-.009				-.012				-.012			

(b) Circumferential distribution of C_p.

Station	Outer shell, external				Outer shell, external				Outer shell, external				Outer shell, external				Outer shell, external			
θ →	198°	216°	234°	252°	198°	216°	234°	252°	198°	216°	234°	252°	198°	216°	234°	252°	198°	216°	234°	252°
0.5	0.218	0.224	0.224	0.213	0.170	0.179	0.177	0.165	0.020	0.028	0.028	0.013	-0.191	-0.183	-0.181	-0.200	-0.241	-0.238	-0.237	-0.242
14.0	.004	0	0	.003	-.003	-.005	-.005	0	-.009	-.013	-.012	-.008	-.017	-.019	-.019	-.016	-.019	-.022	-.022	-.018
43.0	-.006	-.005	-.008	-.008	-.009	-.007	-.009	-.010	-.010	-.009	-.010	-.012	-.012	-.012	-.013	-.014	-.013	-.012	-.013	-.014

[redacted]

TABLE V - EXTERNAL AND INTERNAL PRESSURE COEFFICIENTS OF NACA 8-INCH RAM-JET CONFIGURATION FOR FOUR ANGLES OF ATTACK AT FREE-STREAM MACH NUMBER OF 1.99 - Continued

Station	$\alpha = 3^\circ$; $m_3/m_0 = 0.999$				$\alpha = 3^\circ$; $m_3/m_0 = 0.909$				$\alpha = 3^\circ$; $m_3/m_0 = 0.607$				$\alpha = 3^\circ$; $m_3/m_0 = 0.289$				$\alpha = 6^\circ$; $m_3/m_0 = 0.995$			
	(a) Continued. Longitudinal distribution of C_p.																			
	Outer shell			Center body	Outer shell			Center body	Outer shell			Center body	Outer shell			Center body	Outer shell			Center body
	External		Internal		External		Internal		External		Internal		External		Internal		External		Internal	
$\theta \rightarrow$	180°	270°	0°	0°	180°	270°	0°	0°	180°	270°	0°	0°	180°	270°	0°	0°	180°	270°	0°	0°
-1.0				0.556				0.554				1.314				1.437				0.640
-0.5				.566				.553				1.406				1.495				.639
0				.557				.998				1.428				1.561				.640
0.5	0.133	0.208	0.629	.280	0.048	0.169	1.264	.980	-0.162	-0.074	1.546	1.332	-0.246	-0.220	1.670	1.577	0.061	0.210	0.384	.339
1.0	.090	.154	.627	.400	.056	.135	1.261	1.805	-.078	.006	1.529	1.487	-.214	-.149	1.658	1.641	.027	.154	.541	.626
1.5	.063	.123	.457	.344	.041	.105	1.276	1.269	-.045	.029	1.534	1.524	-.166	-.069	1.658	1.655	.006	.125	.409	.288
2.0	.048	.098	.305	.074	.031	.083	1.286	1.290	-.029	.028	1.537	1.537	-.102	-.047	1.660	1.661	-.002	.097	.358	.033
2.5	.038	.087	.390	.475	.021	.073	1.294	1.304	-.026	.033	1.541	1.545	-.084	-.025	1.663	1.663	-.009	.085	.324	.340
3.0	.025	.070	.254	.358	.007	.069	1.307	1.307	-.029	.024	1.546	1.548	-.075	-.020	1.665	1.663	-.019	.069	.193	.311
4.0	.008	.048	.372	.292	-.007	.041	1.313	1.326	-.033	.017	1.551	1.558	-.062	-.009	1.667	1.667	-.033	.042	.284	.250
5.0	.002	.033	.351	.433	-.010	.028	1.316	1.321	-.031	.004	1.557	1.561	-.052	-.016	1.668	1.670	-.031	.026	.344	.333
6.0	-.010	.016	.542	.377	-.021	.012	1.314	1.300	-.040	-.010	1.561	1.558	-.055	-.025	1.671	1.670	-.036	.006	.773	.716
7.0	-.020	.004	.615	.578	-.031	0	1.300	1.298	-.048	-.019	1.561	1.561	-.057	-.031	1.672	1.671	-.041	-.007	.794	.796
8.0	-.017	0	.760	.746	-.025	-.002	1.311	1.293	-.038	-.019	1.569	1.581	-.048	-.089	1.675	1.674	-.034	-.014	.834	.813
9.0	-.019	-.007	.790	.826	-.024	-.012	1.302	1.323	-.036	-.026	1.570	1.577	-.044	-.036	1.677	1.677	-.031	-.025	.799	.829
10.0	-.026	-.015		.804	-.038	-.014		1.325	-.049	-.026		1.595	-.055	-.036		1.679	-.038	-.028		.796
11.0	-.013	-.013		.624	-.021	-.017		1.340	-.031	-.029		1.587	-.056	-.038		1.680	-.020	-.029		.610
12.0	-.008	-.011		.484	-.016	-.012		1.368	-.025	-.025		1.598	-.030	-.033		1.681	-.014	-.031		.538
14.0	-.005	-.010		.996	-.010	-.012		1.425	-.019	-.021		1.613	-.023	-.029		1.685	-.006	-.033		1.018
16.0	-.001	-.005		1.121	-.007	-.010		1.470	-.014	-.020		1.629	-.018	-.026		1.689	-.002	-.035		1.128
18.0	.005	-.002		1.209	.002	-.007		1.507	-.004	-.016		1.643	-.007	-.021		1.691	-.009	-.035		1.207
21.0	.014	-.002		1.320	.014	-.007		1.561	.010	-.012		1.665	.009	-.016		1.695	.024	-.034		1.307
24.0	.014	.008		1.411	.007	.005		1.610	.001	-.002		1.685	-.002	-.004		1.699	-.007	-.026		1.393
27.0	-.008	0		1.480	-.012	-.002		1.650	-.018	-.009		1.701	-.030	-.012		1.704	-.010	-.026		1.460
31.0	.004			1.529	.002			1.675	-.008			1.711	-.004			1.704	.004			1.508
35.0	-.016				-.020				-.024				-.025				-.021			
37.0				1.576				1.711				1.721				1.706				1.553
40.0	-.008				-.009				-.012				-.012				-.006			
45.0	-.005				-.007				-.009				-.009				-.005			
	(b) Continued. Circumferential distribution of C_p.																			
Station	Outer shell, external				Outer shell, external				Outer shell, external				Outer shell, external				Outer shell, external			
$\theta \rightarrow$	198°	216°	234°	252°	198°	216°	234°	252°	198°	216°	234°	252°	198°	216°	234°	252°	198°	216°	234°	252°
0.5	0.146	0.161	0.175	0.188	0.067	0.091	0.110	0.130	-0.155	-0.137	-0.114	-0.107	-0.245	-0.241	-0.233	-0.233	0.076	0.101	0.129	0.163
14.0	-.007	-.010	-.008	-.008	-.012	-.016	-.015	-.012	-.021	-.025	-.025	-.023	-.025	-.029	-.029	-.028	-.011	.025	-.033	-.038
43.0	-.006	-.008	-.012	-.015	-.007	-.010	-.014	-.016	-.010	-.012	-.016	-.019	-.012	-.012	-.016	-.020	-.010	-.016	-.024	-.035

[redacted]

[redacted]

TABLE V - EXTERNAL AND INTERNAL PRESSURE COEFFICIENTS OF NACA 8-INCH RAM-JET CONFIGURATION FOR FOUR ANGLES OF ATTACK AT FREE-STREAM MACH NUMBER OF 1.99 - Concluded

NACA

(a) Concluded. Longitudinal distribution of C_p.

Station	$\alpha = 6^\circ$; $m_3/m_0 = 0.975$				$\alpha = 6^\circ$; $m_3/m_0 = 0.871$				$\alpha = 10^\circ$; $m_3/m_0 = 0.955$				$\alpha = 10^\circ$; $m_3/m_0 = 0.851$			
	Outer shell			Center body	Outer shell			Center body	Outer shell			Center body	Outer shell			Center body
	External		Internal		External		Internal		External		Internal		External		Internal	
$\theta \rightarrow$	180°	270°	0°	0°	180°	270°	0°	0°	180°	270°	0°	0°	180°	270°	0°	0°
-1.0				0.639				0.638				0.758				0.757
-0.5				.639				.638				.785				.785
0				.640				1.274				.778				.863
0.5	0.029	0.218	0.699	.477	-0.052	0.154	1.210	.912	-0.024	0.218	0.248	.423	-0.170	0.178	0.879	.785
1.0	.012	.164	.869	.608	-.029	.135	1.240	1.197	-.053	.163	.442	.560	-.141	.157	1.062	1.006
1.5	-.007	.131	1.027	1.114	-.026	.113	1.283	1.274	-.067	.128	.357	.232	-.130	.131	1.168	1.167
2.0	-.016	.104	1.129	1.141	-.029	.090	1.304	1.306		.100	.344	-.006		.108	1.216	1.215
2.5	-.024	.092	1.169	1.165	-.034	.080	1.318	1.323		.084	.256	.074		.092	1.246	1.247
3.0	-.031	.075	1.188	1.183	-.042	.062	1.332	1.333		.065	.141	.314		.074	1.269	1.269
4.0	-.042	.047	1.202	1.210	-.062	.041	1.344	1.356		.033	.466	.242		.042	1.297	1.307
5.0	-.041	.030	1.203	1.205	-.049	.024	1.352	1.358	-.067	.012	.688	.722	-.094	.020	1.314	1.321
6.0	-.045	.009	1.200	1.184	-.052	.006	1.354	1.344	-.060	-.009	.804	.780	-.082	-.005	1.326	1.317
7.0	-.049	-.006	1.194	1.189	-.066	-.010	1.347	1.347	.001	-.027	.824	.807	-.004	-.023	1.331	1.329
8.0	-.036	-.012	1.214	1.194	-.042	-.016	1.361	1.347	-.038	-.036	.847	.829	-.056	-.034	1.345	1.331
9.0	-.034	-.024	1.223	1.258	-.038	-.025	1.358	1.378	-.034	-.046	.845	.870	-.047	-.048	1.351	1.364
10.0	-.043	-.030		1.262	-.060	-.028		1.384	-.041	-.048		.861	-.056	-.048		1.370
11.0	-.024	-.033		1.274	-.029	-.034		1.396	-.019	-.062		.902	-.052	-.062		1.384
12.0	-.017	-.031		1.309	-.023	-.036		1.417	-.012	-.067		.968	-.024	-.069		1.405
14.0	-.010	-.033		1.377	-.014	-.038		1.460	-.008	-.079		1.079	-.014	-.082		1.444
16.0	-.004	-.036		1.433	-.007	-.040		1.498	.006	-.089		1.166	-.007	-.093		1.478
18.0	.006	-.036		1.480	.002	-.038		1.527	.017	-.096		1.231	.008	-.099		1.509
21.0	.021	-.035		1.543	.016	-.038		1.567	.018	-.106		1.314	.006	-.110		1.551
24.0	.003	-.028		1.599	.001	-.029		1.605	.006	-.111		1.394	-.002	-.116		1.589
27.0	-.011	-.026		1.640	-.014	-.028		1.640	-.006	-.110		1.445	-.009	-.116		1.620
31.0	.002			1.668	.002			1.661	.012			1.478	.008			1.642
35.0	-.020				-.021				-.016				-.019			
37.0				1.697				1.695				1.606				1.668
40.0	-.006				-.006				.001				-.002			
45.0	-.005				-.006				-.004				-.008			

(b) Concluded. Circumferential distribution of C_p.

Station	Outer shell, external				Outer shell, external				Outer shell, external				Outer shell, external			
$\theta \rightarrow$	198°	216°	234°	252°	198°	216°	234°	252°	198°	216°	234°	252°	198°	216°	234°	252°
0.5	0.063	0.074	0.124	0.164	-0.031	0.005	0.045	0.088	0	0.037	0.083	0.139	-0.147	-0.102	-0.037	0.051
14.0	-.015	-.028	-.035	-.038	-.019	-.029	-.038	-.042	-.014	-.046	-.090	-.102	-.027	-.053	-.096	-.111
43.0	-.011	-.016	-.024	-.036	-.012	-.017	-.034	-.036	-.028	-.046	-.044	-.056	-.027	-.046	-.046	-.067

[redacted]

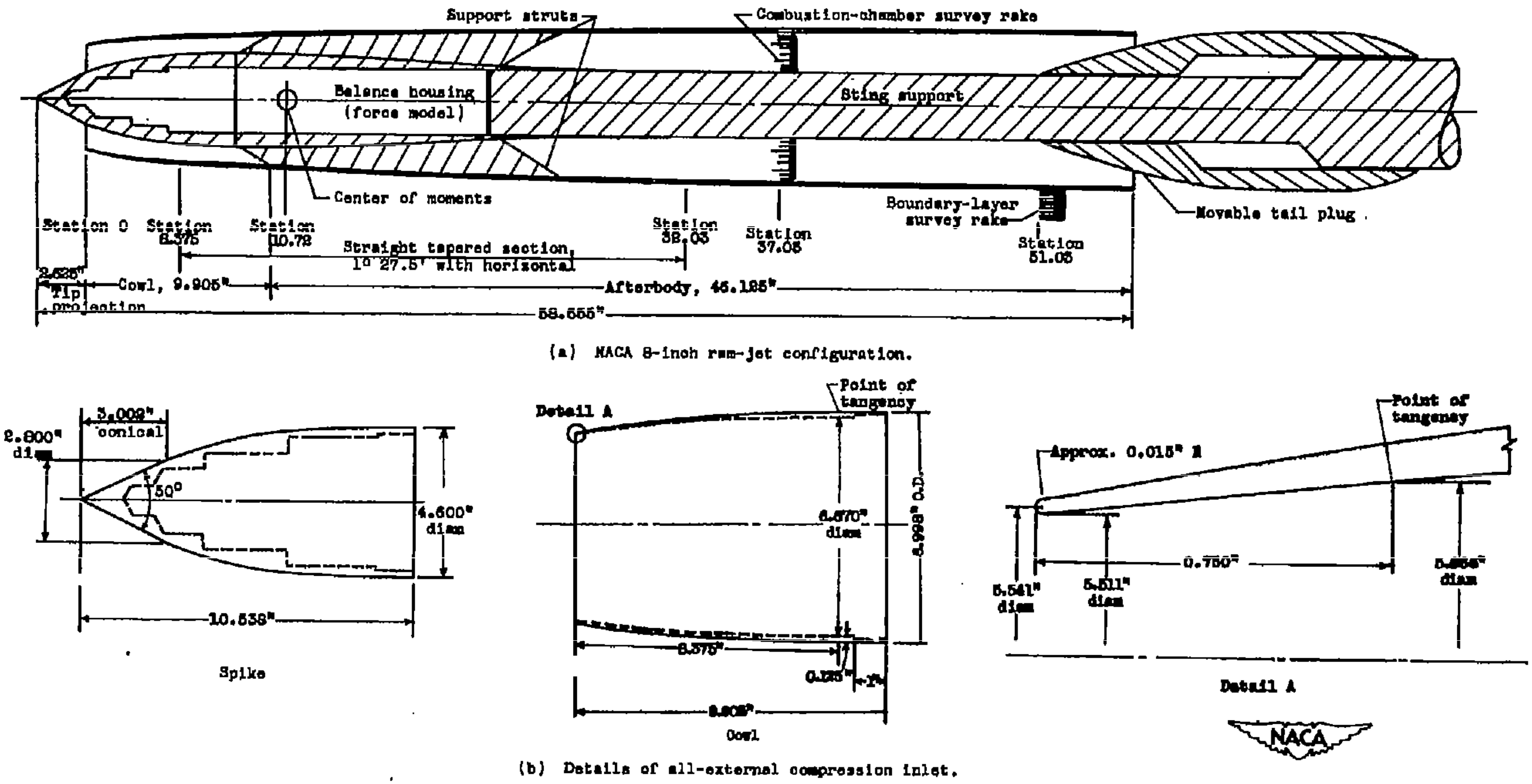

(b) Details of all-external compression inlet.

Figure 1. - Schematic diagram of NACA 8-inch ram-jet configuration showing principal dimensions of model and details of all-external compression inlet.

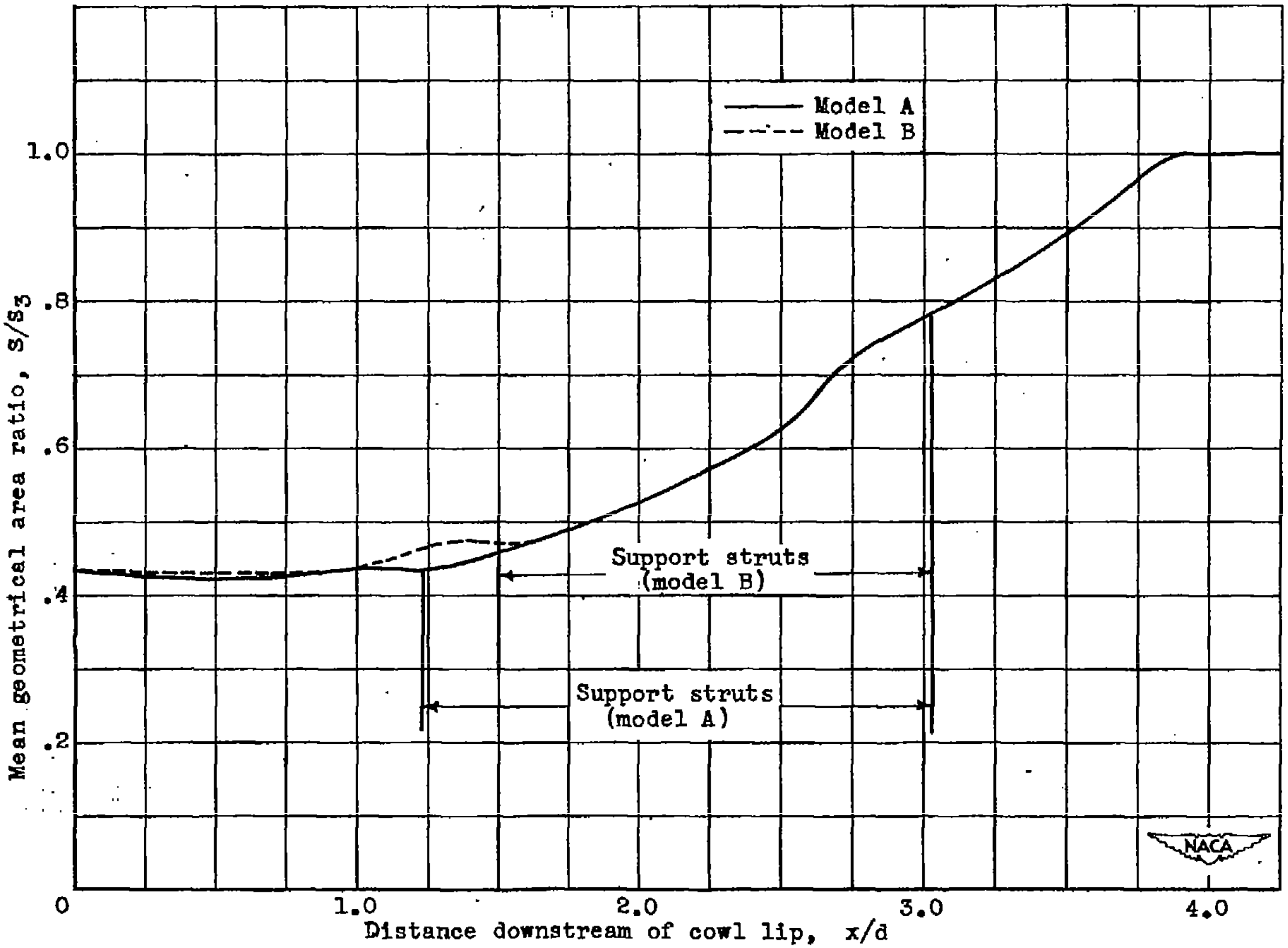

Figure 2. - Longitudinal variation of mean geometrical area.

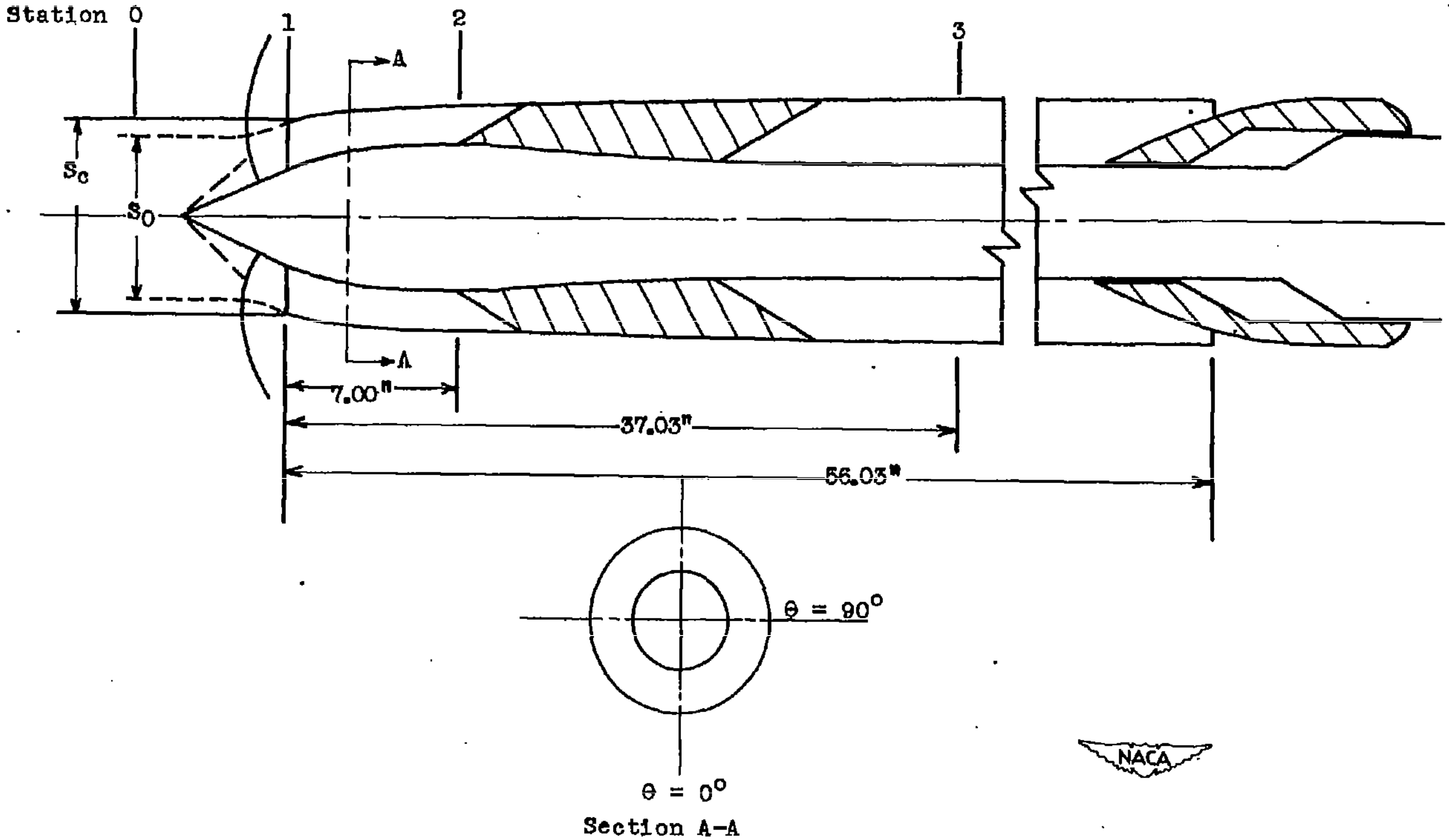

Figure 3. - Notation for 8-inch ram-jet configuration.

2039

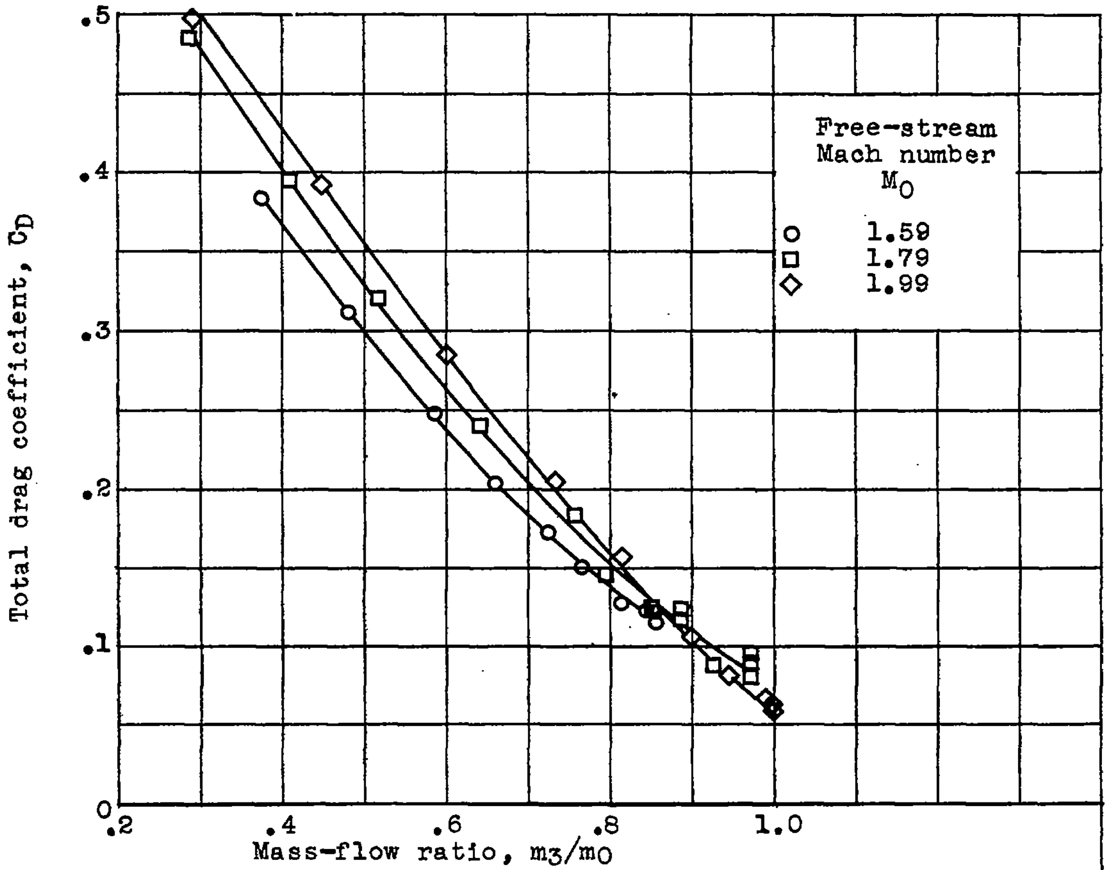

Figure 4. - Variation of total drag coefficient with mass-flow ratio at zero angle of attack for three Mach numbers. Model B.

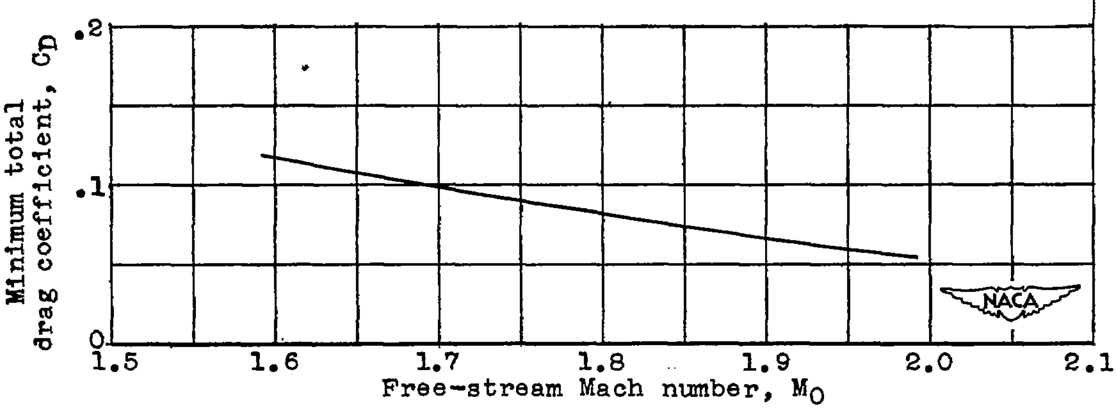

Figure 5. - Variation of minimum drag coefficient with free-stream Mach number at zero angle of attack. Model B.

[redacted]

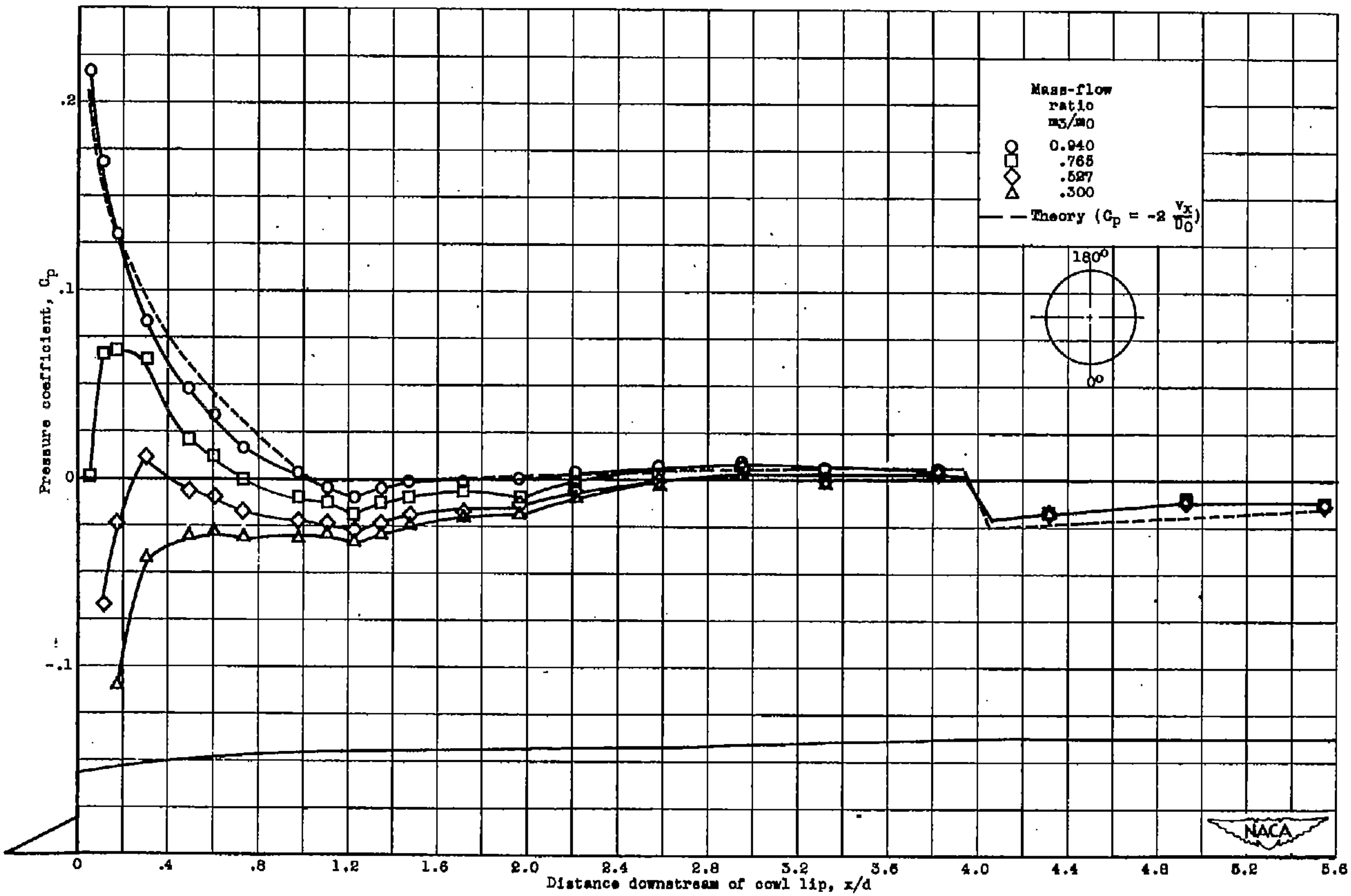

(a) Free-stream Mach number, 1.79.

Figure 6. - Longitudinal variation of external pressure coefficient at zero angle of attack for a range of mass-flow ratios at two Mach numbers. $\theta = 180^\circ$.

[redacted]

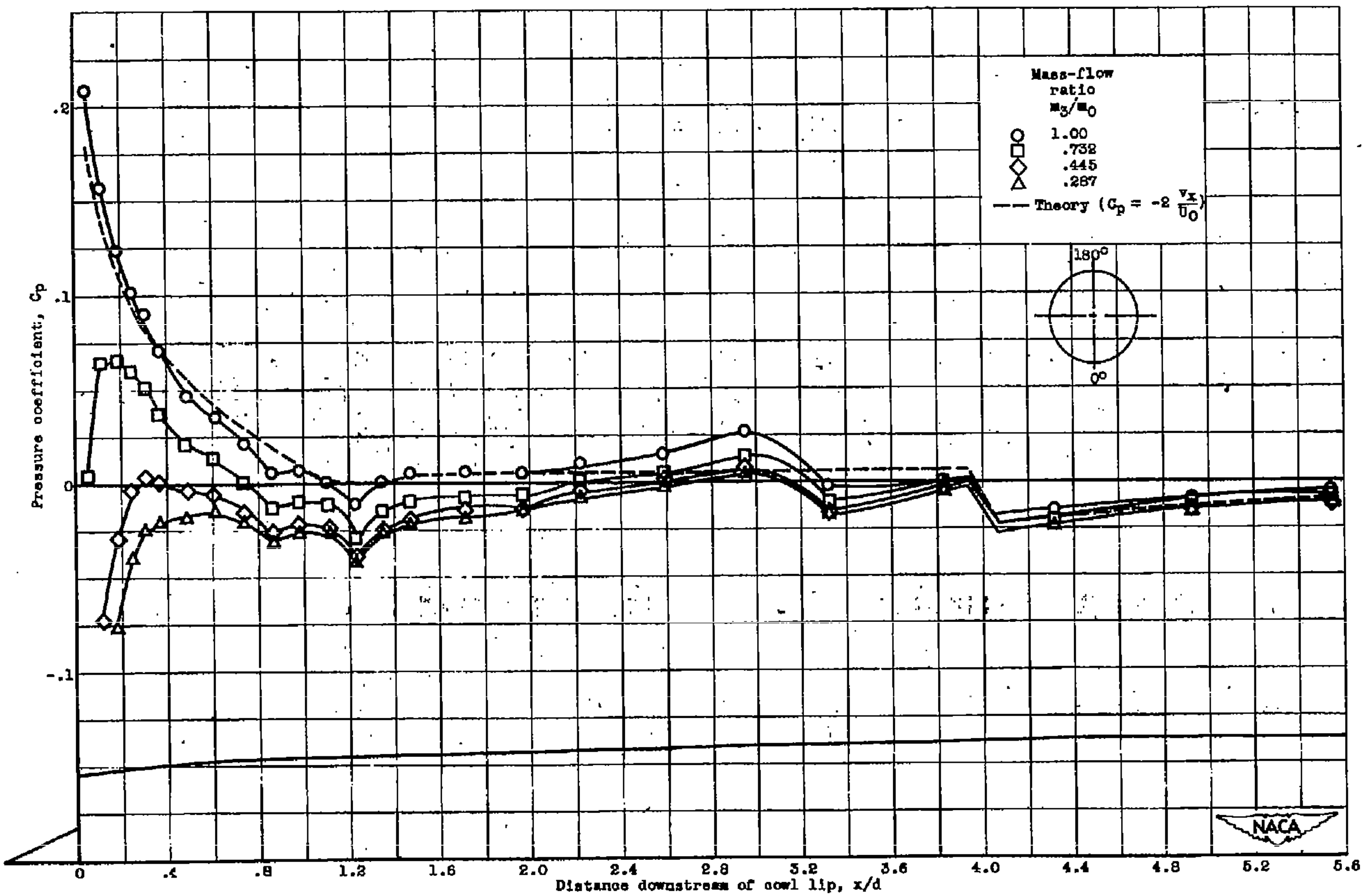

(b) Free-stream Mach number, 1.99.

Figure 6. - Concluded. Longitudinal variation of external pressure coefficient at zero angle of attack for a range of mass-flow ratios at two Mach numbers. θ = 180°.

[redacted]

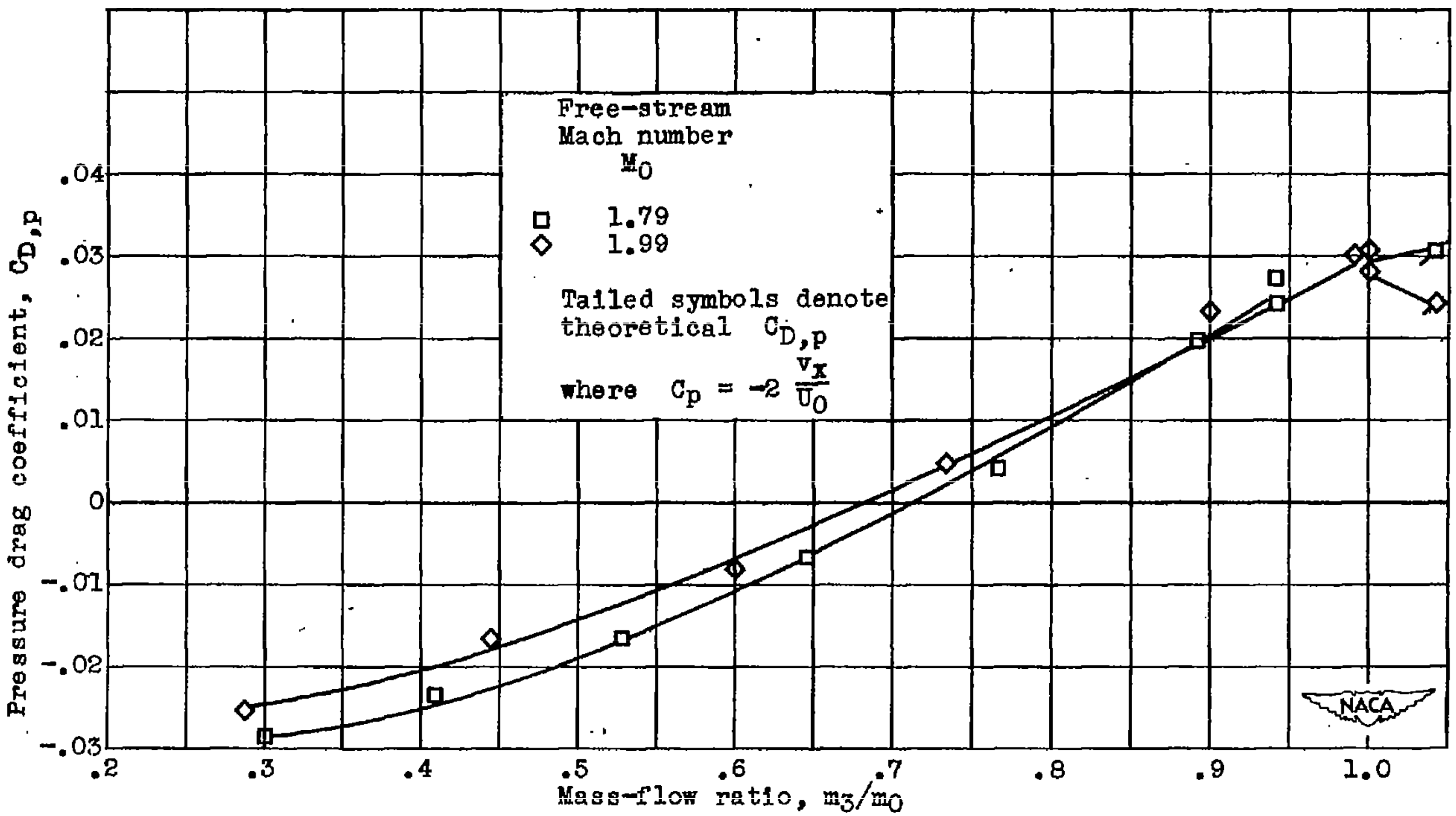

Figure 7. - Variation of pressure drag coefficient with mass-flow ratio at zero angle of attack for two Mach numbers.

[redacted]

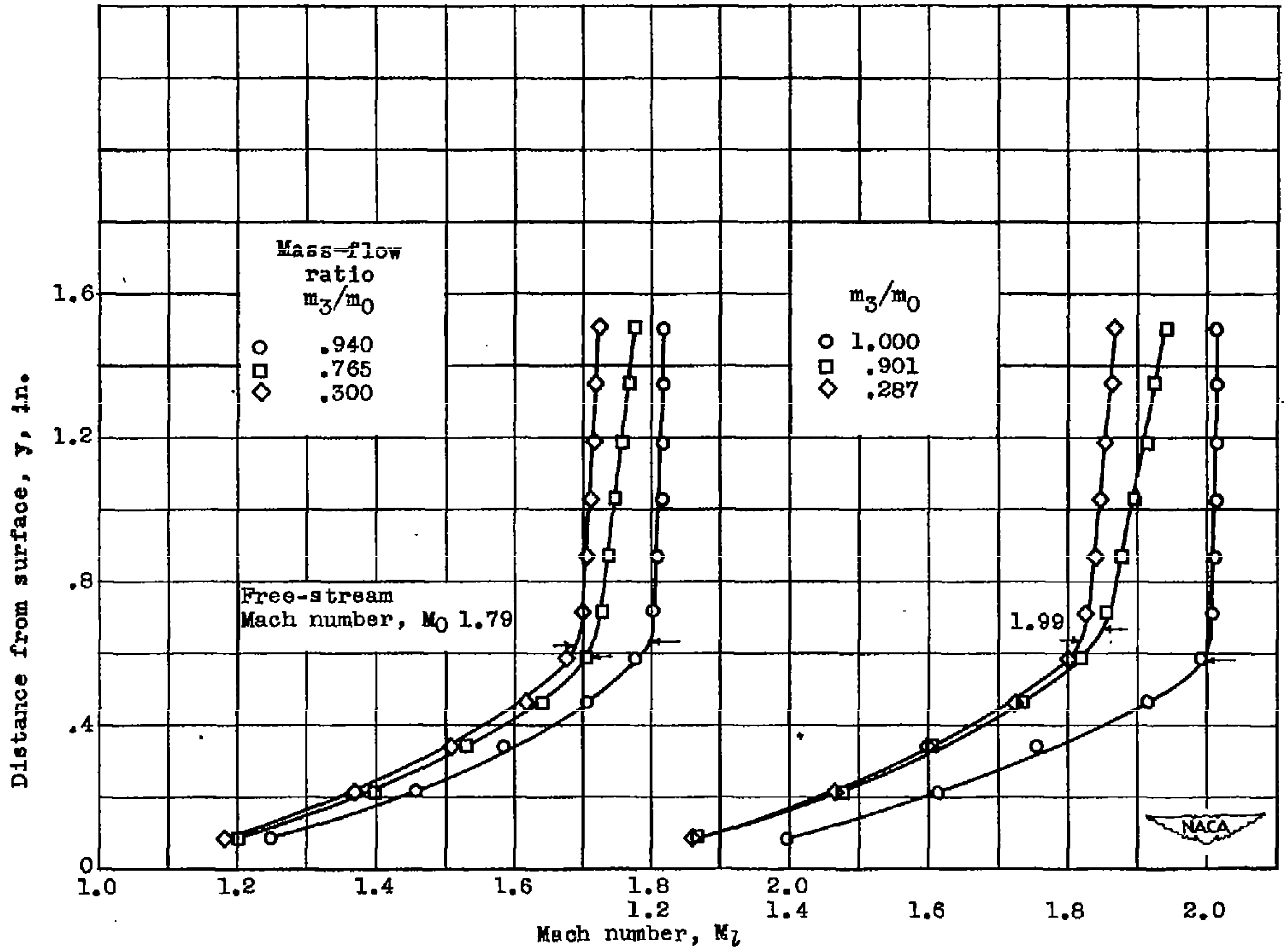

Figure 8. - Variation of Mach-number distribution in boundary layer at zero angle of attack for range of mass-flow ratios at two Mach numbers. Station 51.03.

[redacted]

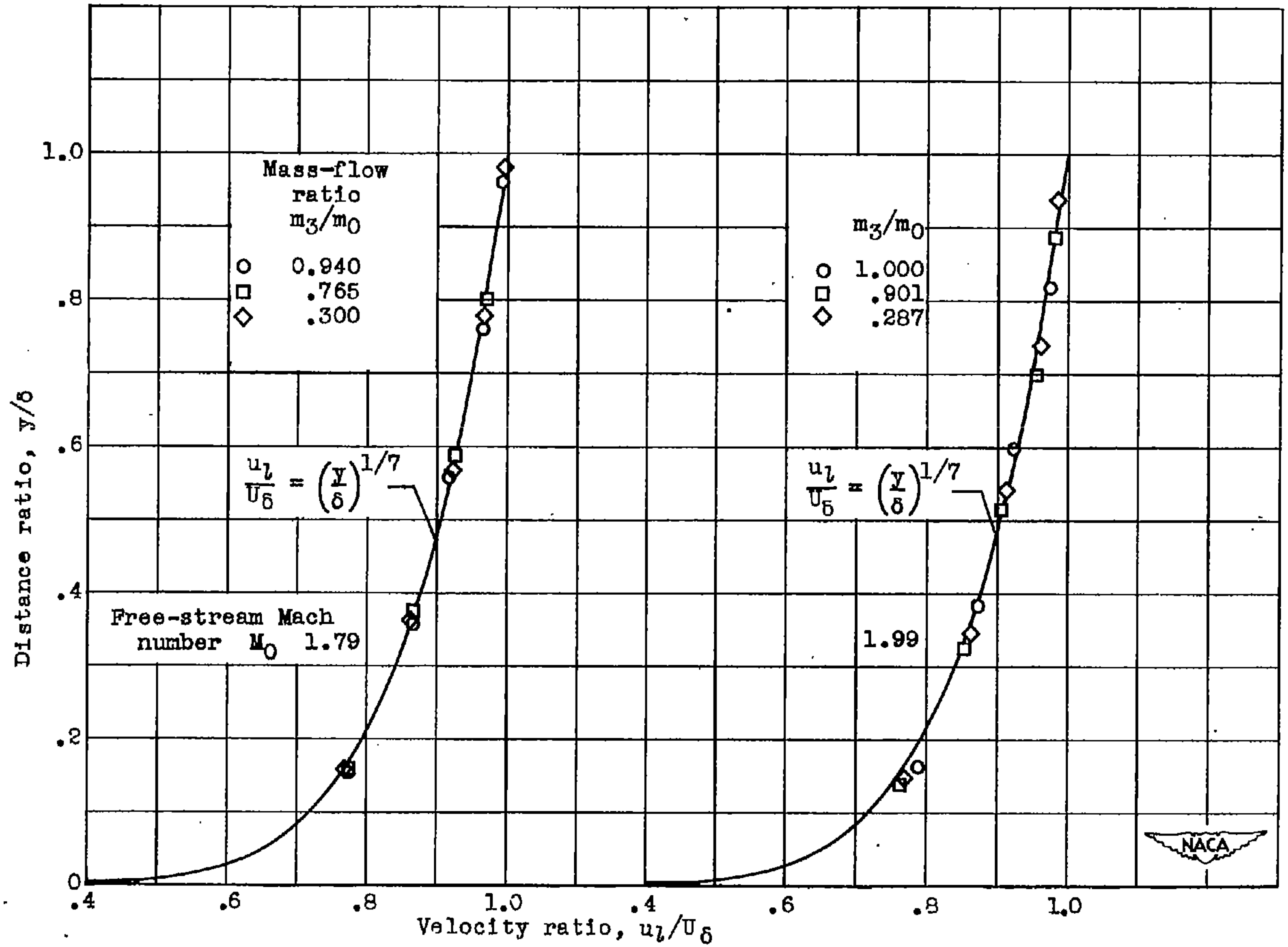

Figure 9. - Comparison of experimental and power-law boundary-layer profiles at zero angle of attack for range of mass-flow ratios and two Mach numbers.

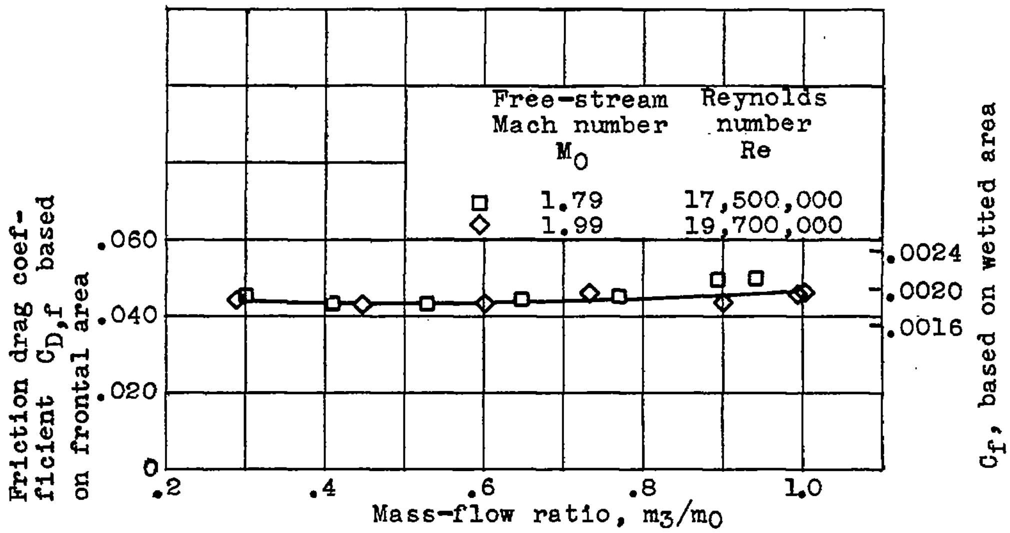

Figure 10. - Variation of friction drag coefficient with mass-flow ratio at zero angle of attack for two Mach numbers.

2039

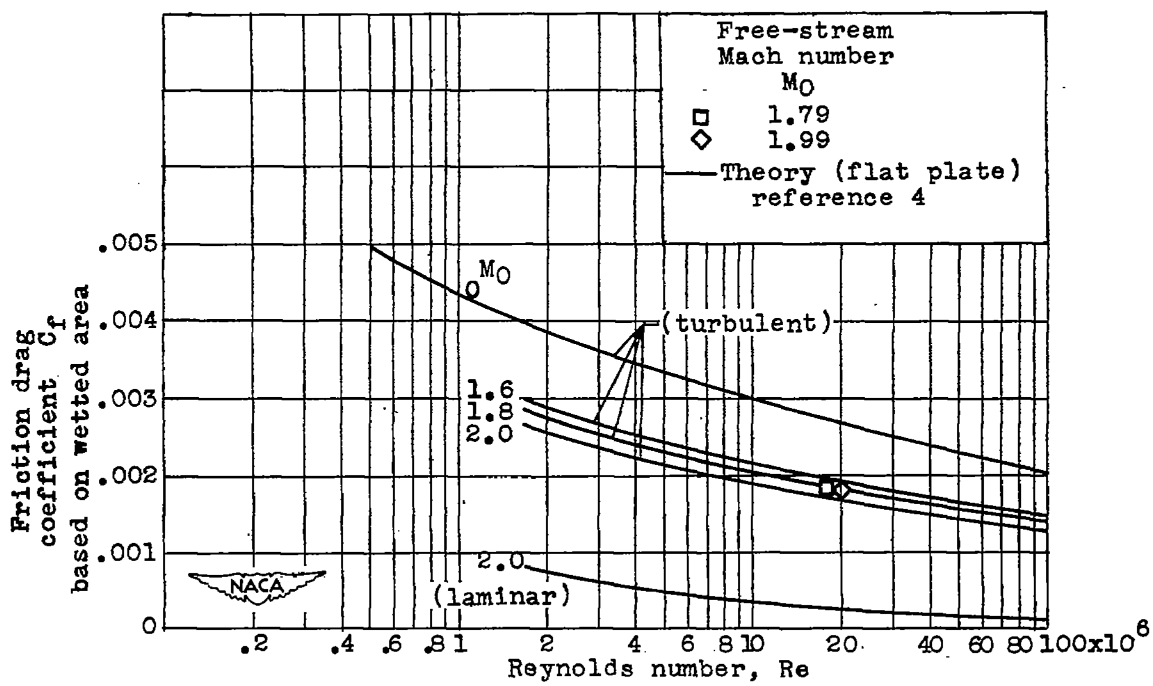

Figure 11. - Comparison of experimental skin-friction drag coefficients with two-dimensional compressible flow theory at two Mach numbers.

2039

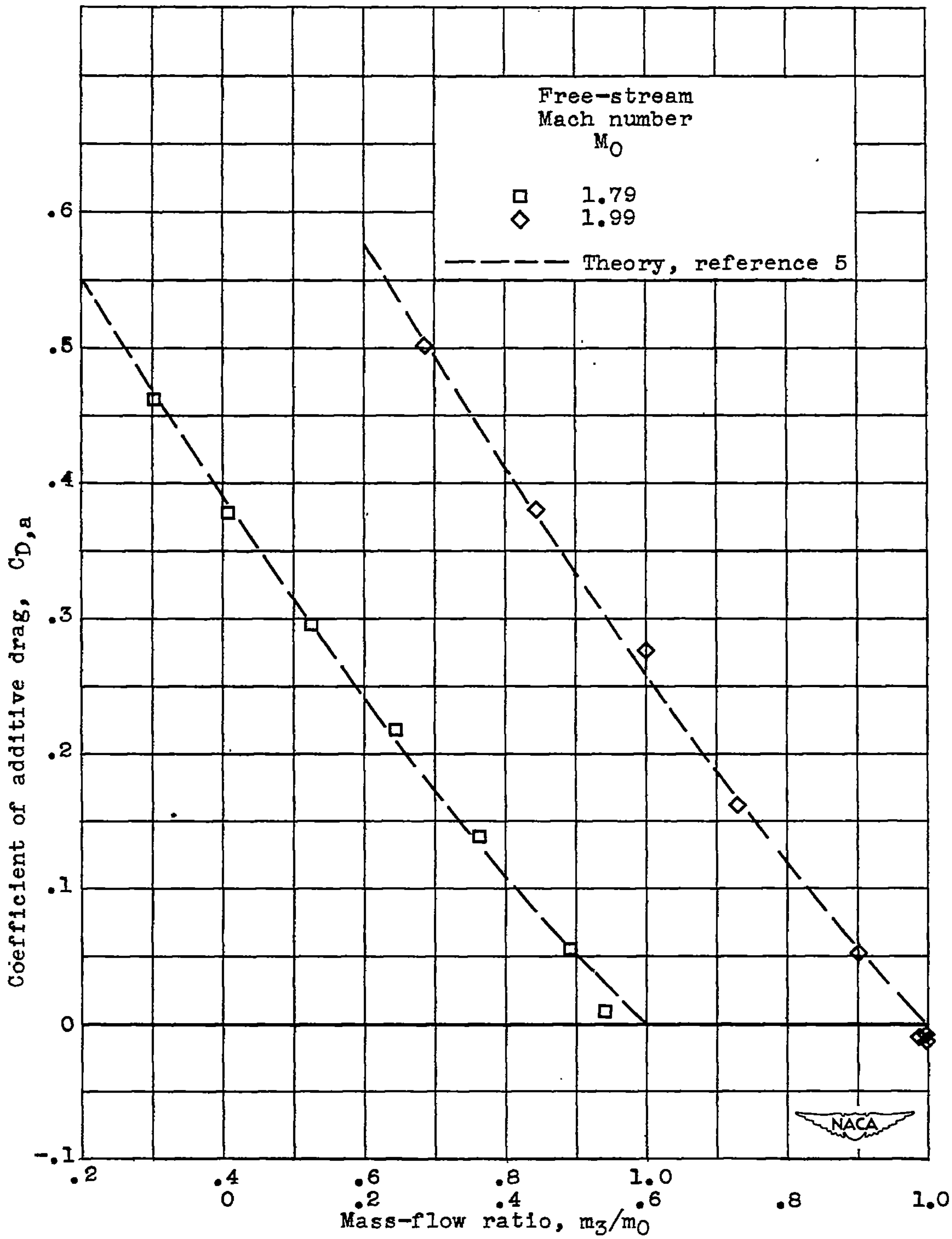

Figure 12. - Comparison of experimental additive drag coefficients with one-dimensional theory for range of mass-flow ratios at two Mach numbers.

2039

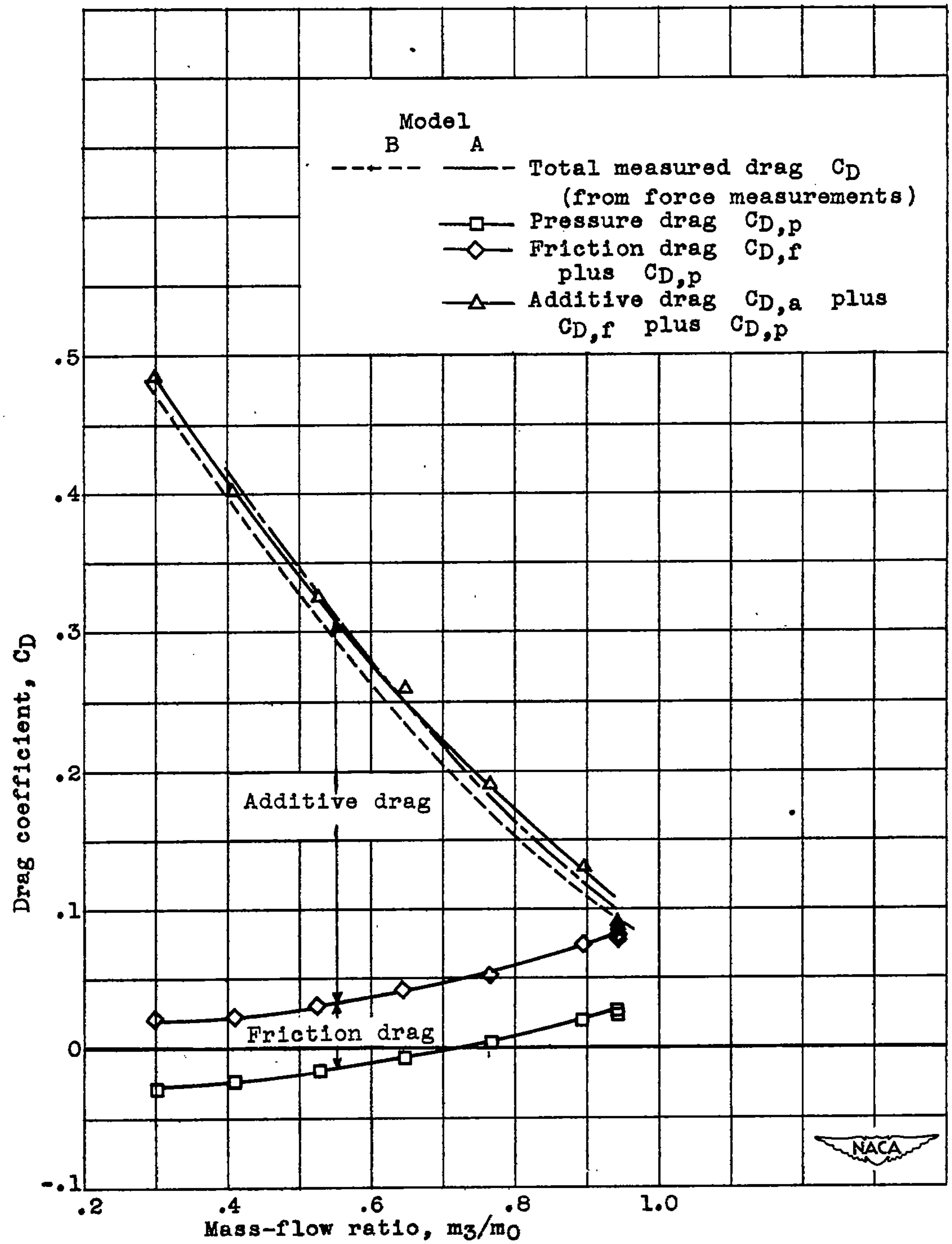

(a) Free-stream Mach number, 1.79.

Figure 13. - Variation of components of total drag coefficients with mass-flow ratio at zero angle of attack for two Mach numbers.

2039

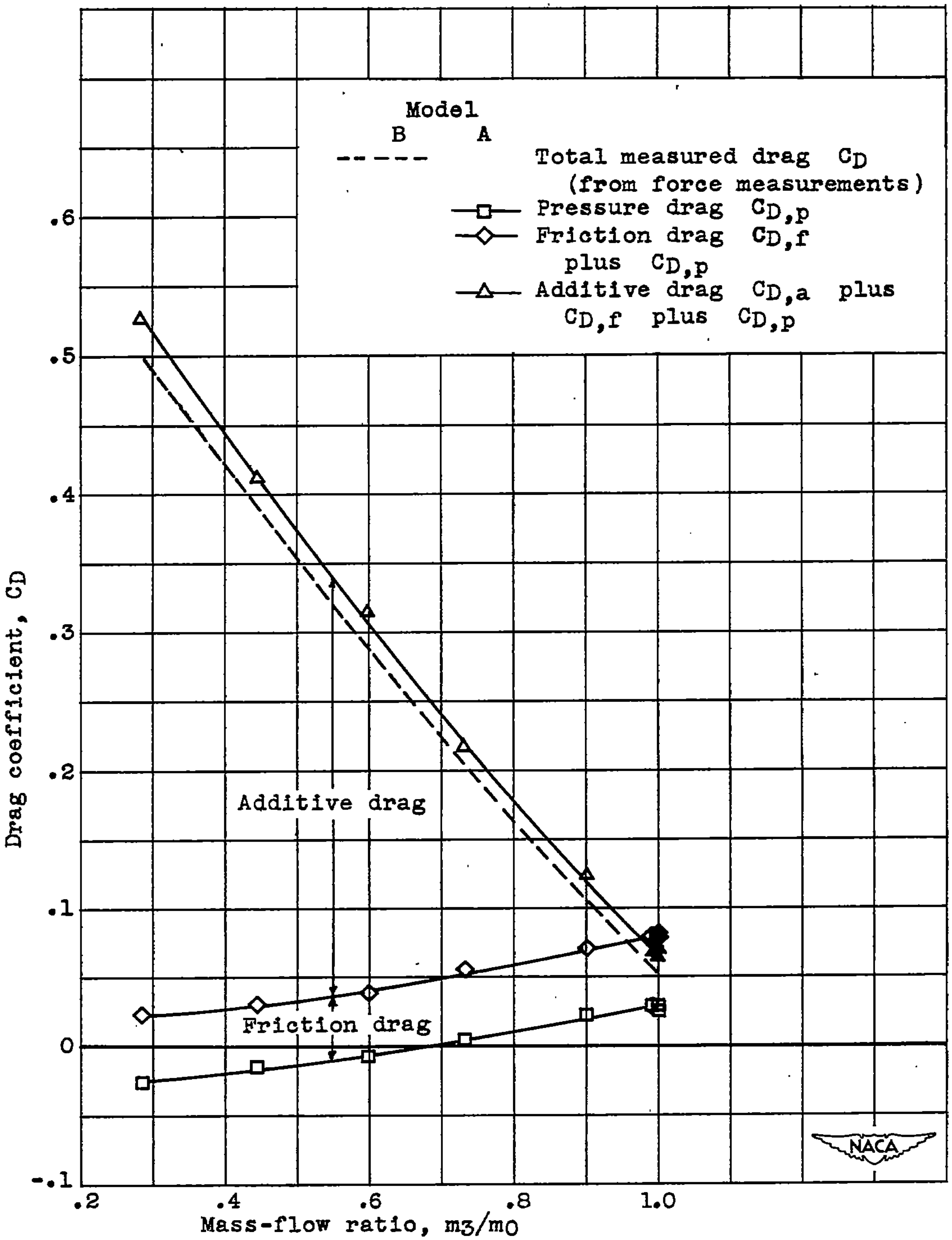

(b) Free-stream Mach number, 1.99.

Figure 13. - Concluded. Variation of components of total drag coefficients with mass-flow ratio at zero angle of attack for two Mach numbers.

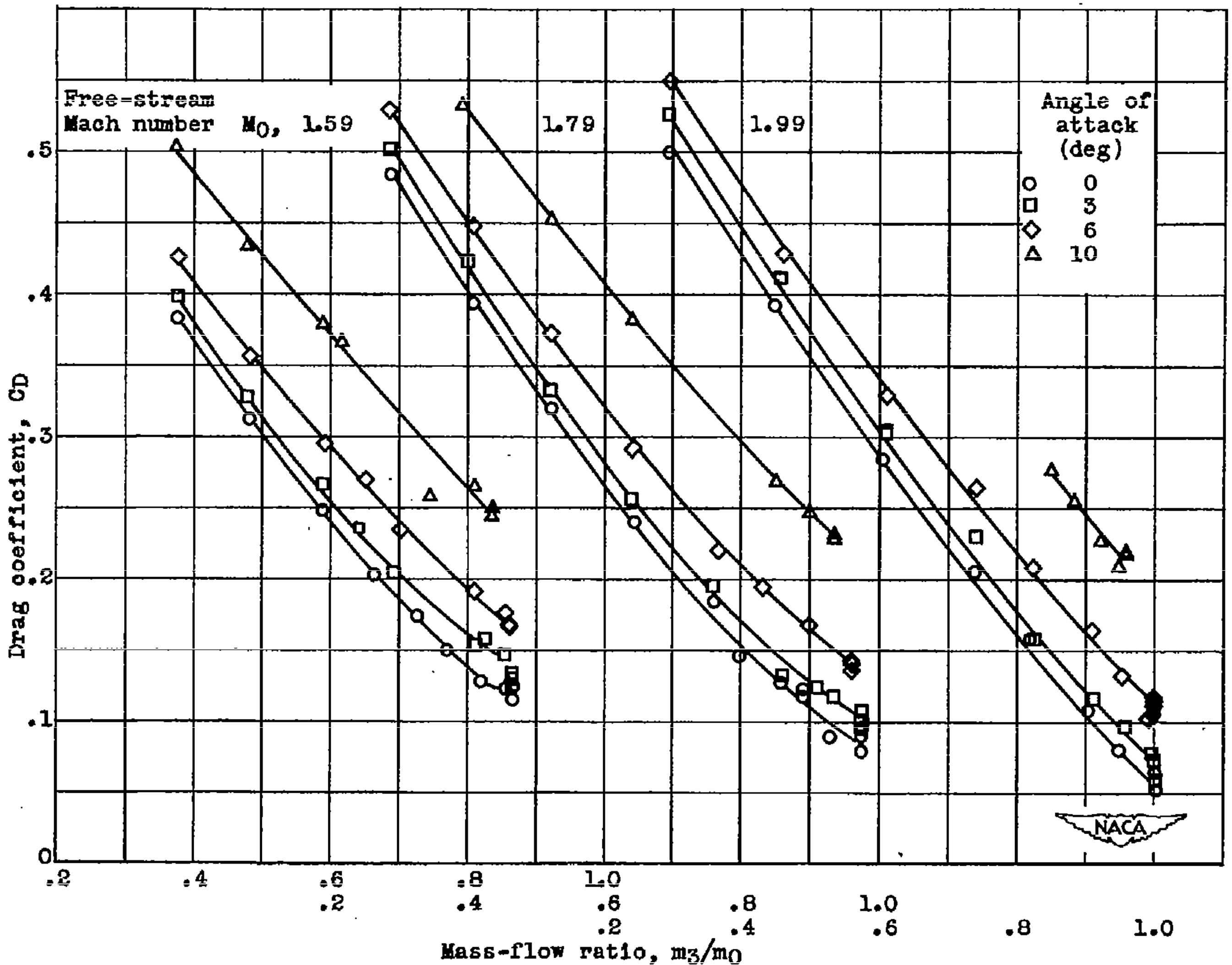

Figure 14. - Variation of total drag coefficient with mass-flow ratio at four angles of attack for three Mach numbers. Model B.

[redacted]

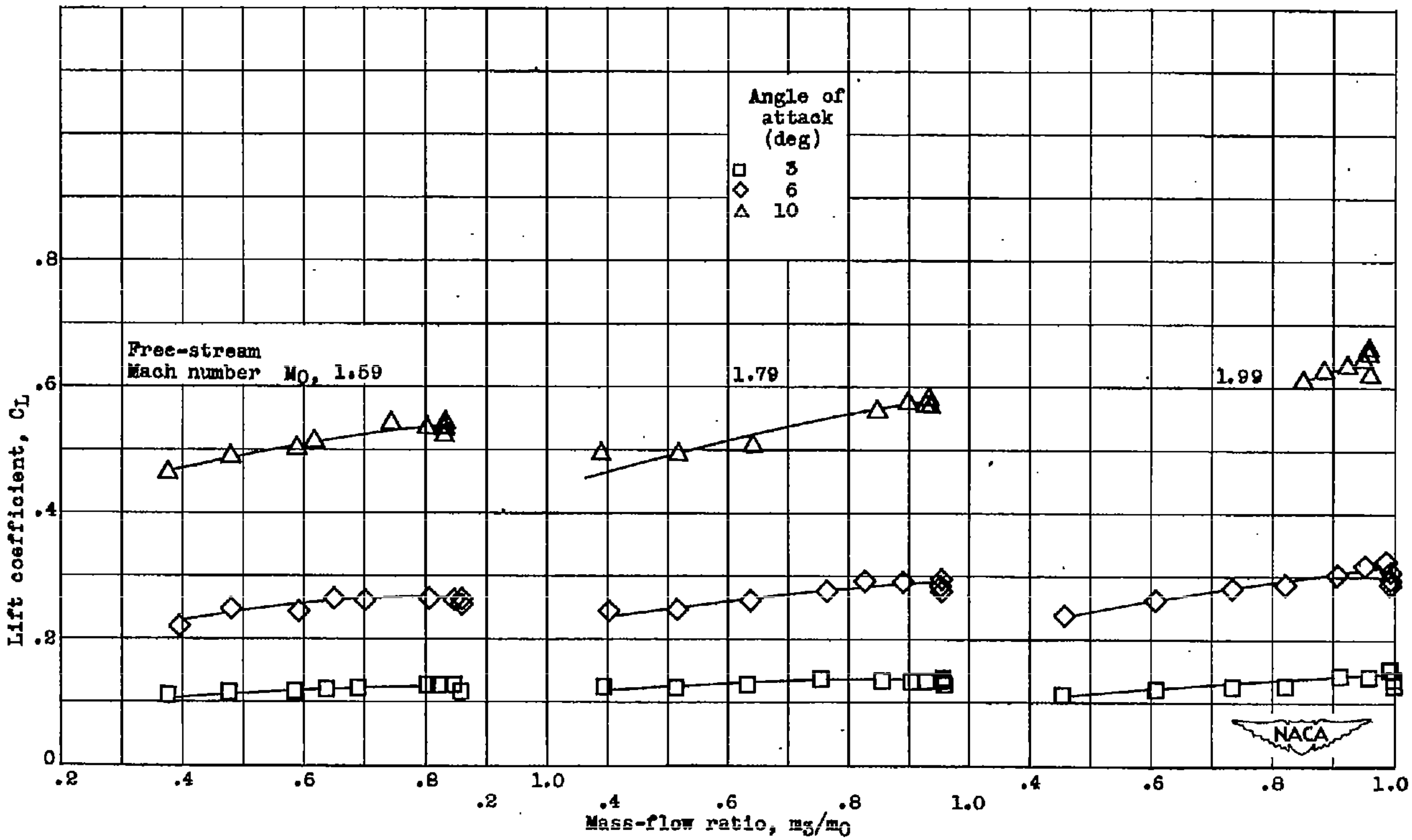

Figure 15. - Variation of external lift coefficients with mass-flow ratio at three angles of attack for three Mach numbers. Model B.

[redacted]

[redacted]

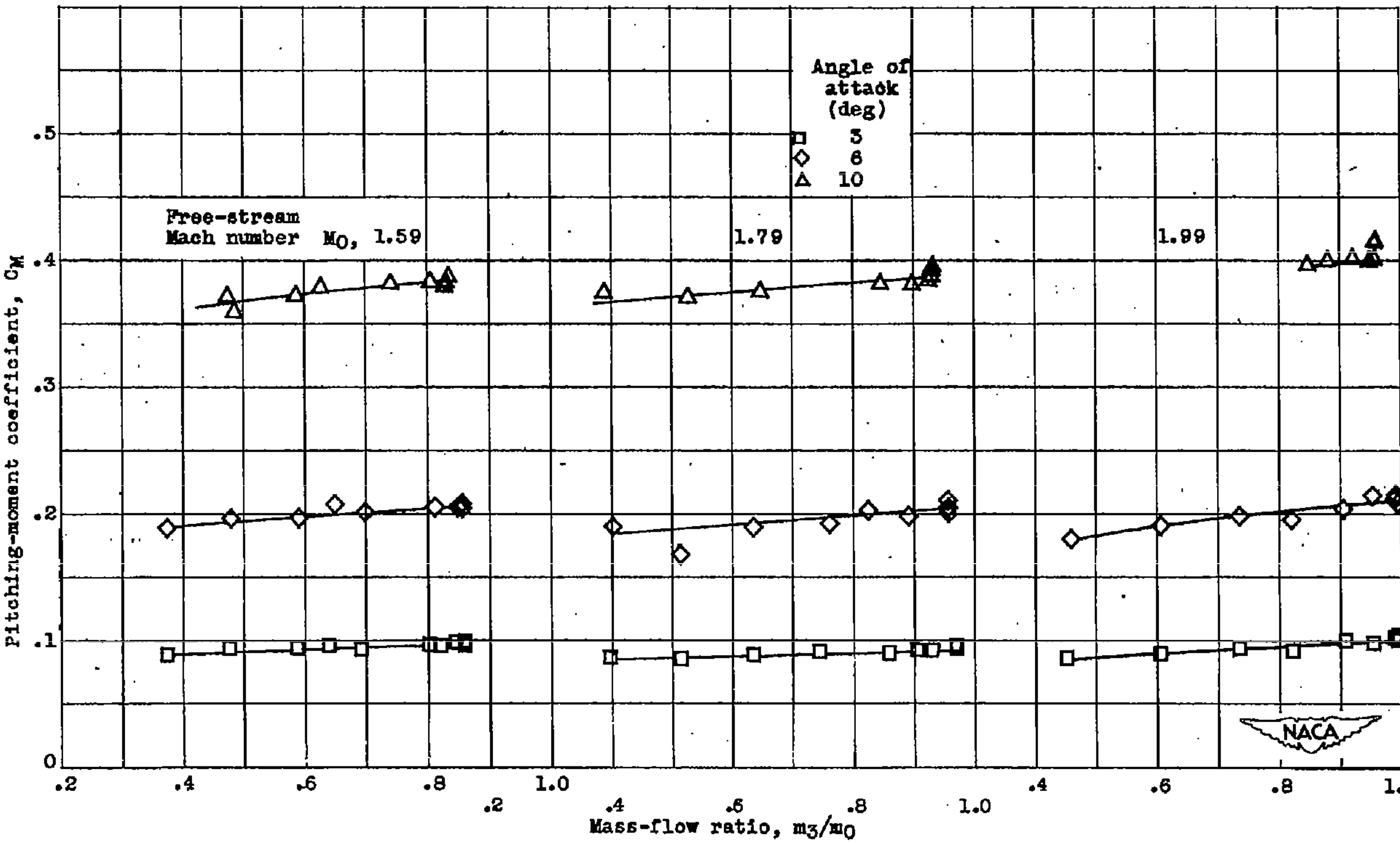

Figure 16. - Variation of pitching-moment coefficient about base of model with mass-flow ratio at three angles of attack for three Mach numbers. Model B.

[redacted]

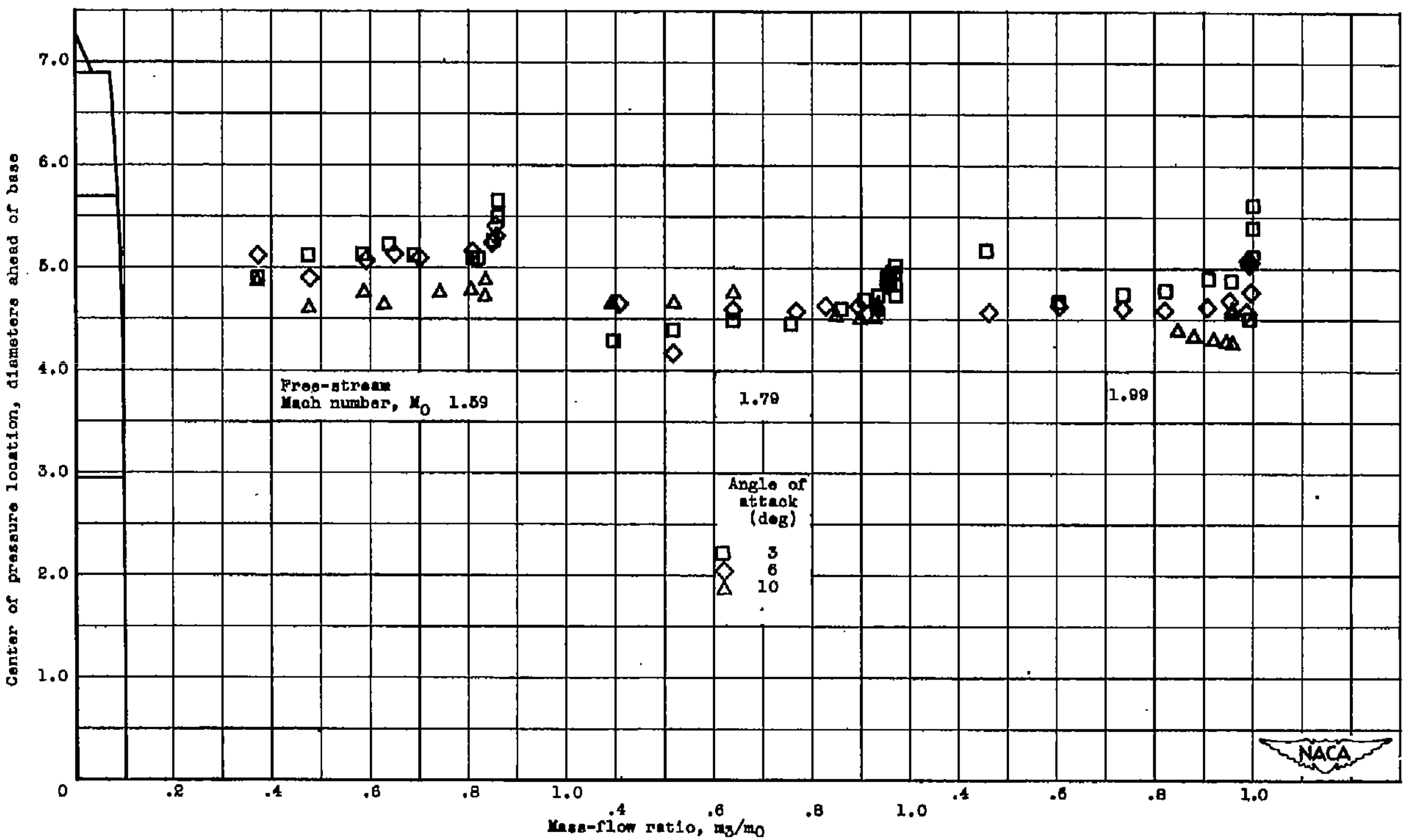

Figure 17. - Variation of center of pressure location with mass-flow ratio at three angles of attack for three Mach numbers. Model B.

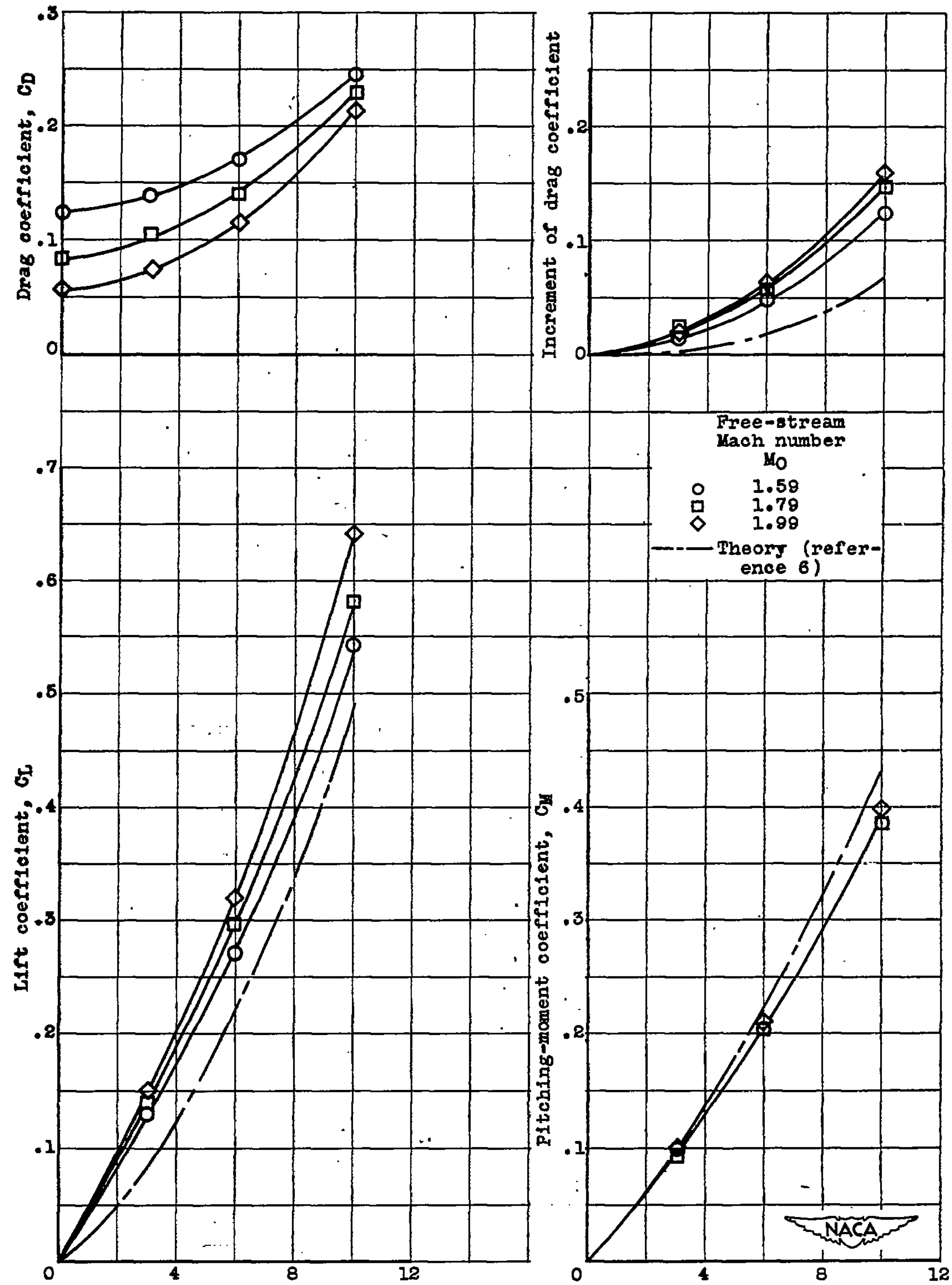

Figure 18. - Variation of external aerodynamic coefficients with angle of attack at critical mass-flow ratios for three Mach numbers. Model B.

2039

2039

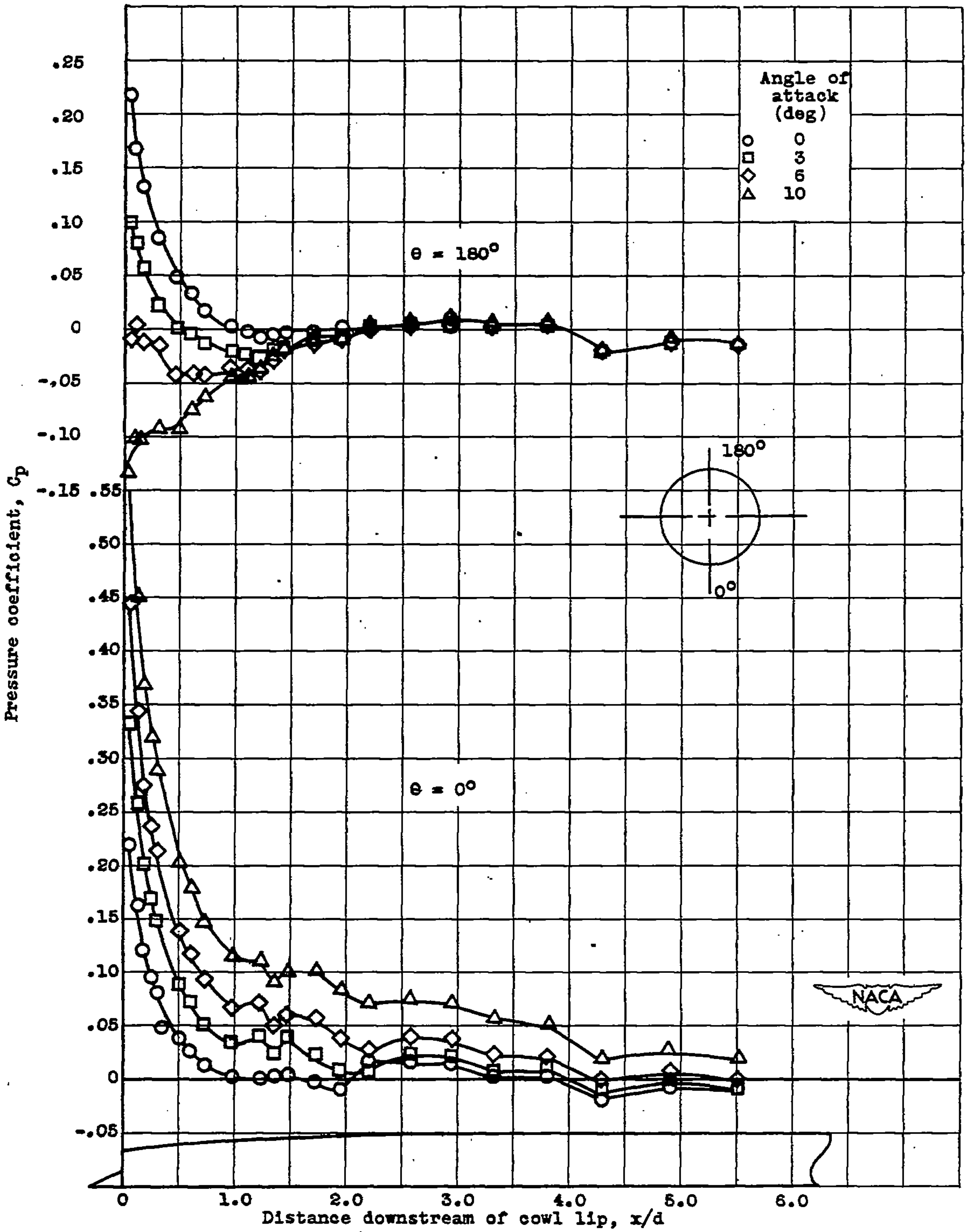

Figure 19. - Longitudinal variation of external pressure coefficients at constant mass-flow ratio of 0.940 for four angles of attack. Free-stream Mach number 1.79.

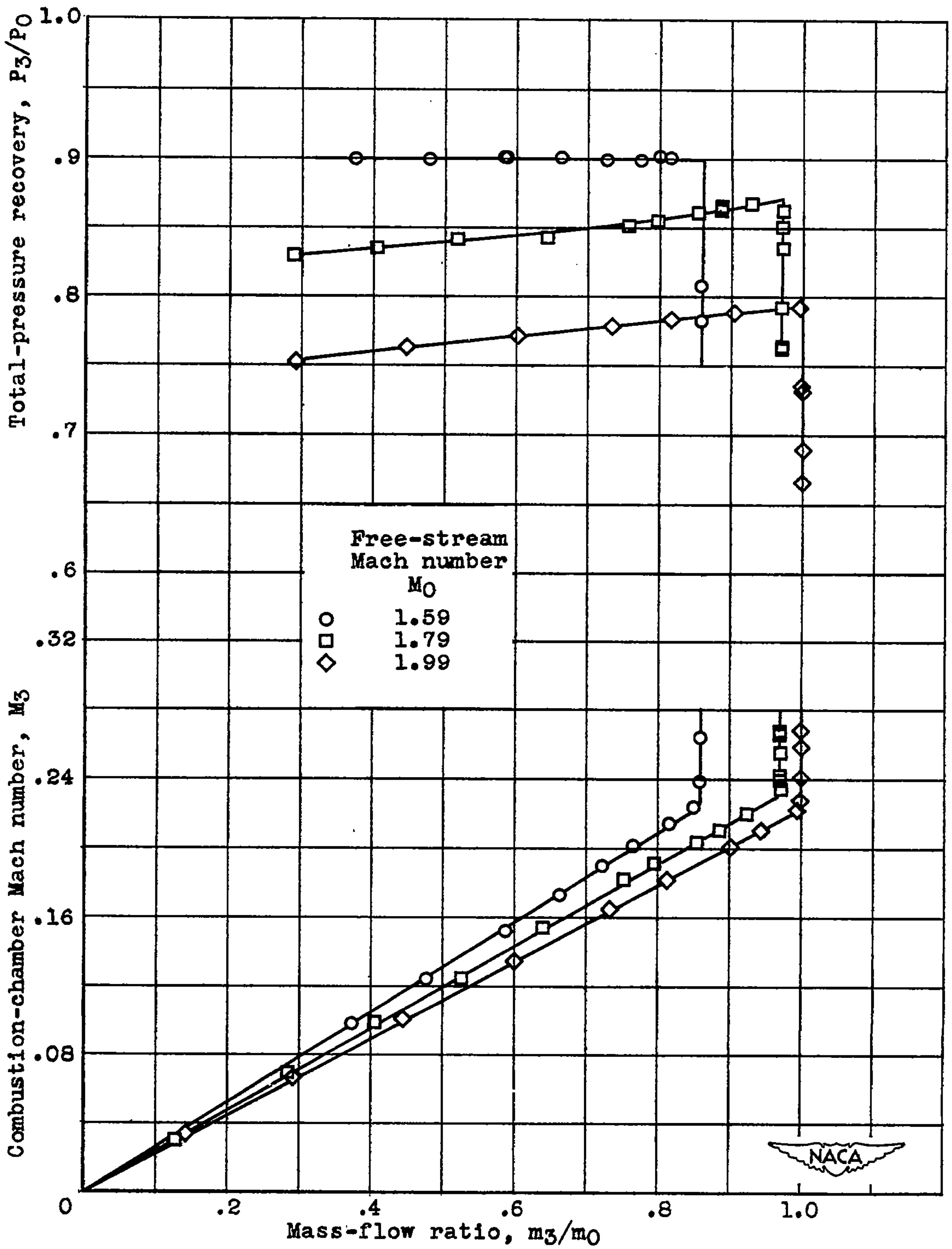

Figure 20. - Variation of total-pressure recovery and combustion-chamber Mach number with mass-flow ratio at zero angle of attack for three Mach numbers. Model B.

2039

2039

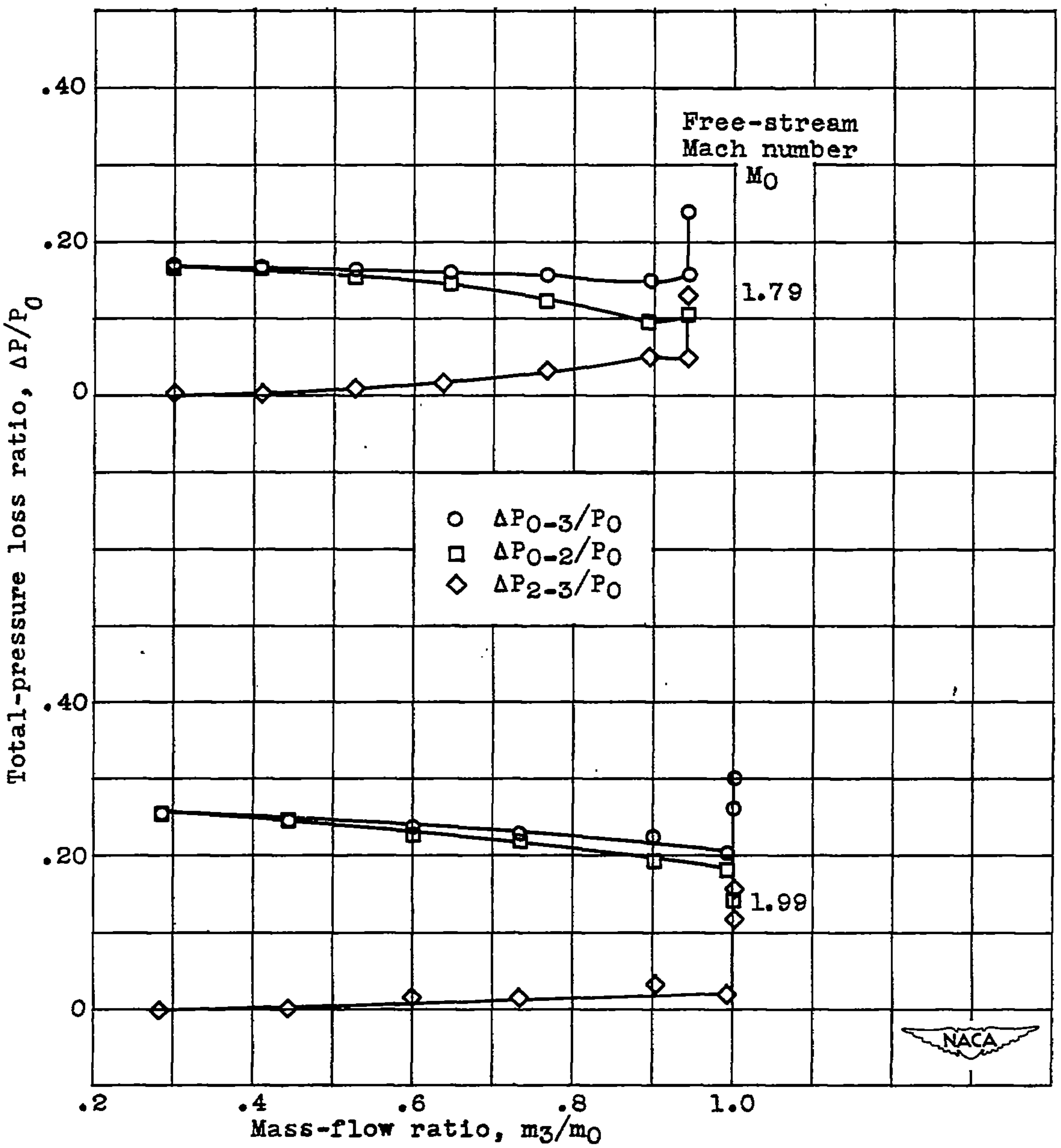

Figure 21. - Variation of components of total-pressure loss with mass-flow ratio at zero angle of attack for two Mach numbers.

2039

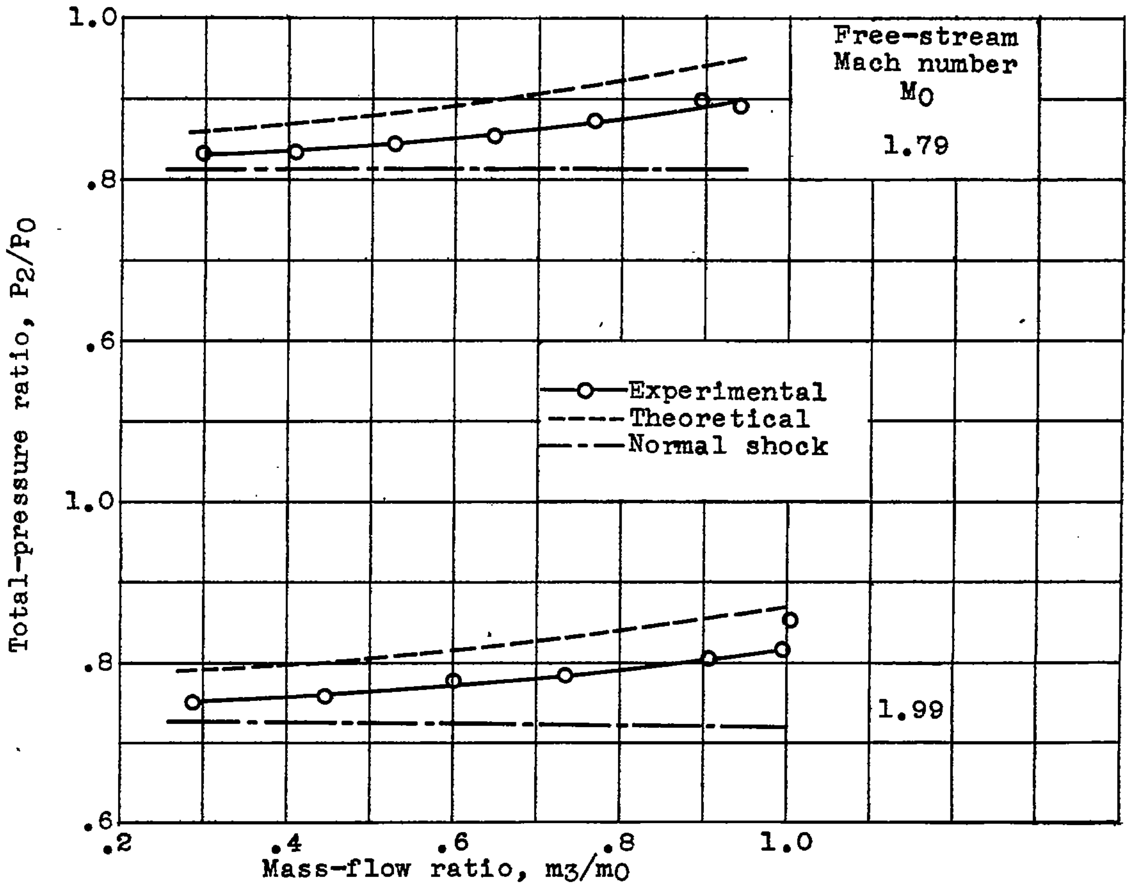

Figure 22. - Comparison of experimental inlet losses with theory at zero angle of attack for range of mass-flow ratios at two Mach numbers.

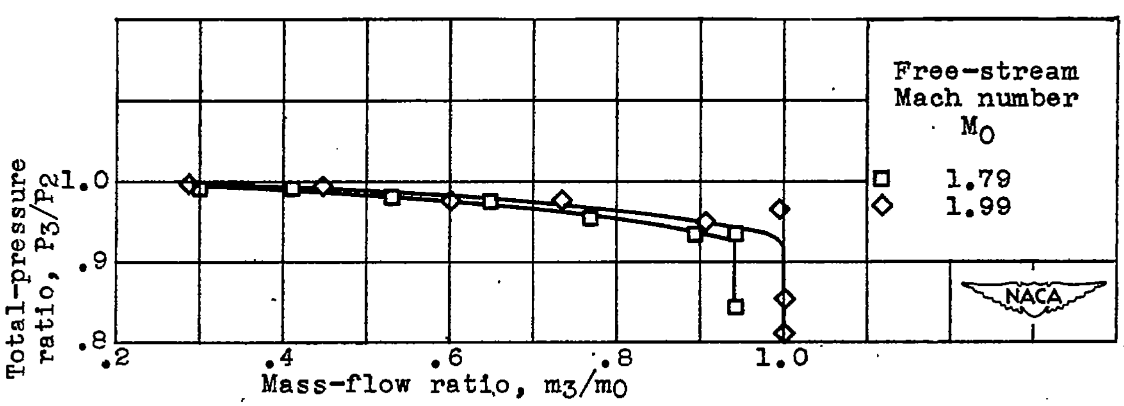

Figure 23. - Variation of subsonic-diffuser recovery with mass-flow ratio at zero angle of attack for two Mach numbers.

2039

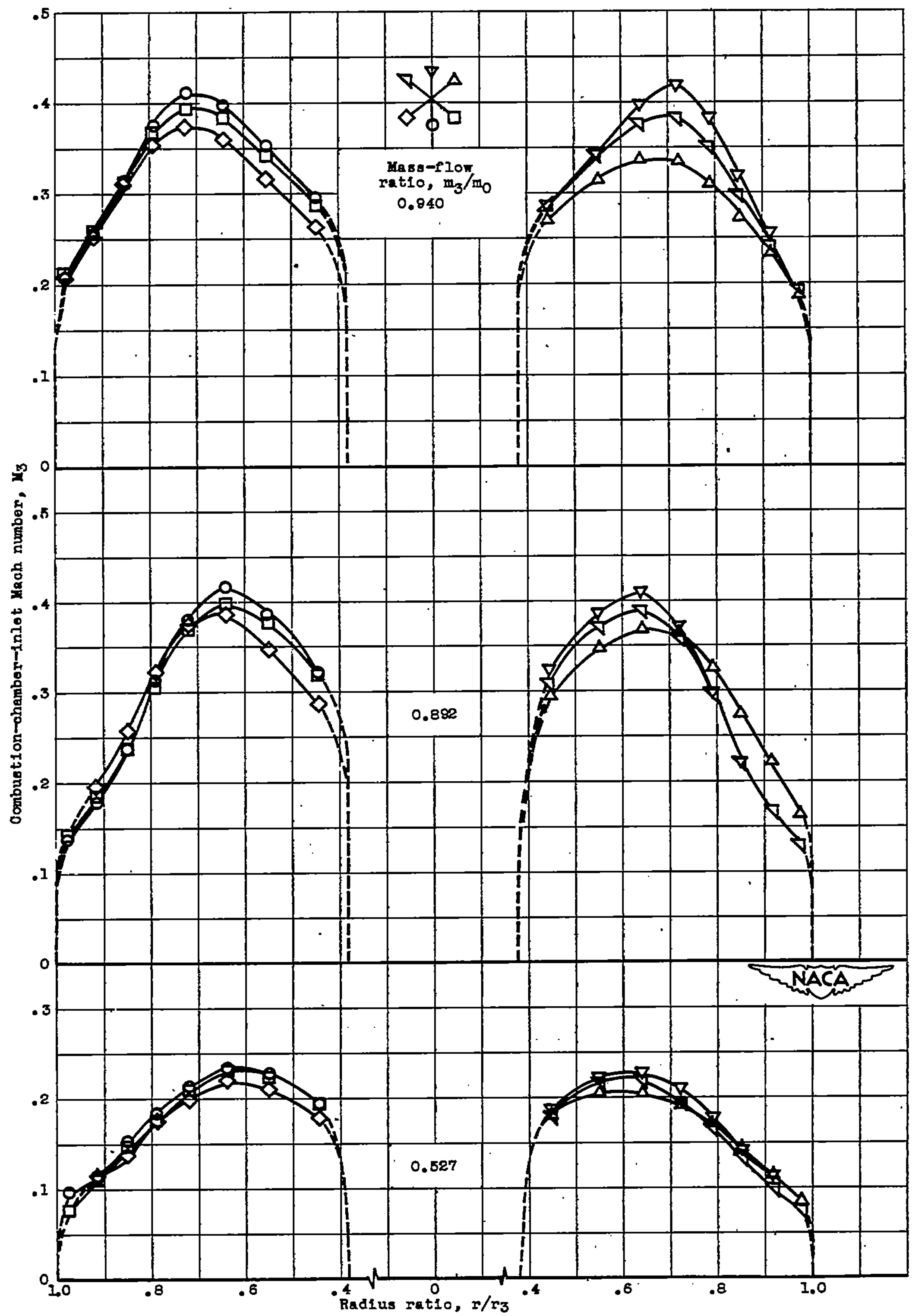

Figure 24. - Variation of Mach number distribution at combustion-chamber inlet for several mass-flow ratios at zero angle of attack. Free-stream Mach number, 1.79.

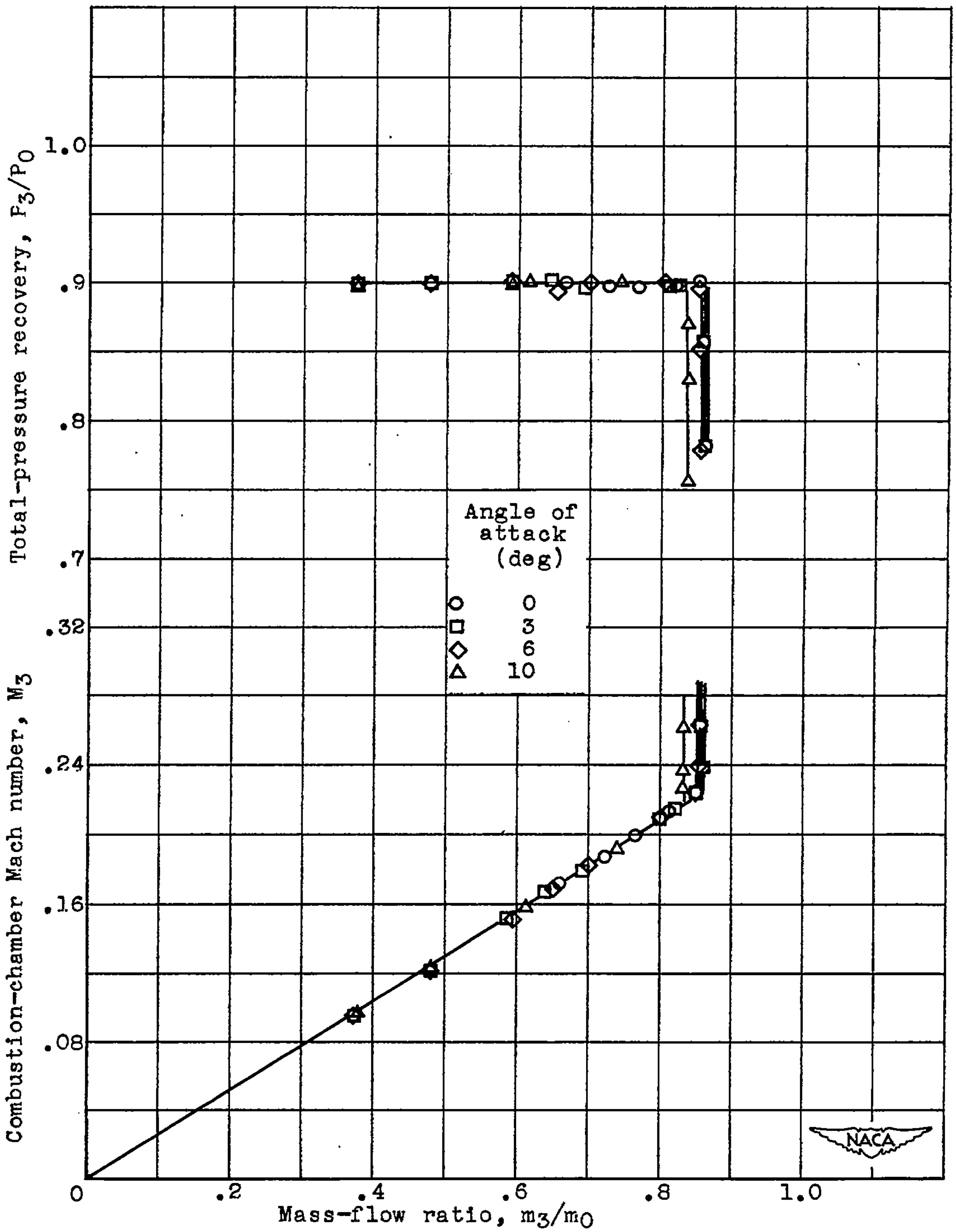

(a) Free-stream Mach number, 1.59.

Figure 25. - Variation of total-pressure recovery and combustion-chamber Mach number with mass-flow ratio at four angles of attack for three Mach numbers. Model B.

2039

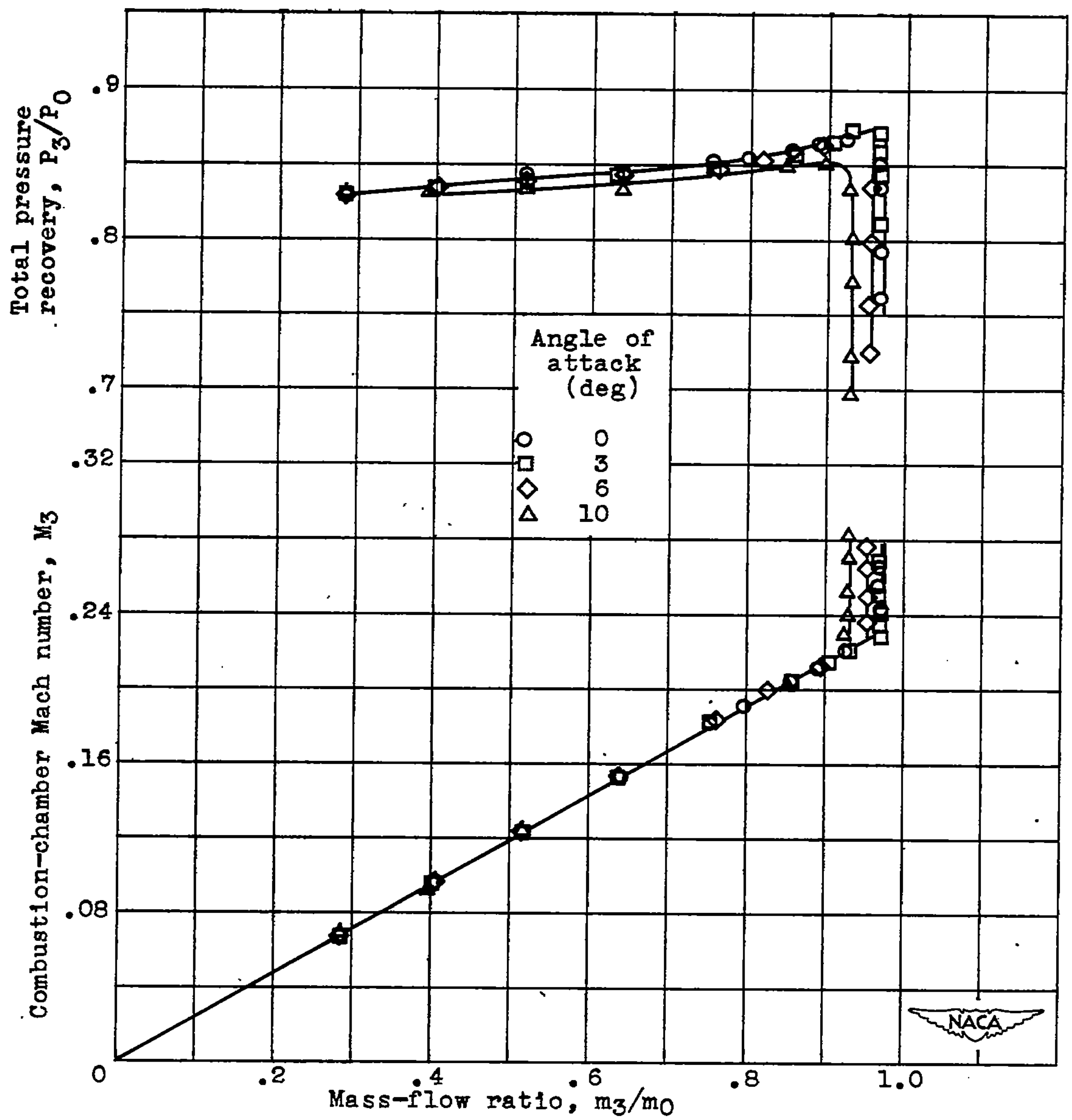

(b) Free-stream Mach number, 1.79.

Figure 25. - Continued. Variation of total-pressure recovery and combustion-chamber Mach number with mass-flow ratio at four angles of attack for three Mach numbers. Model B.

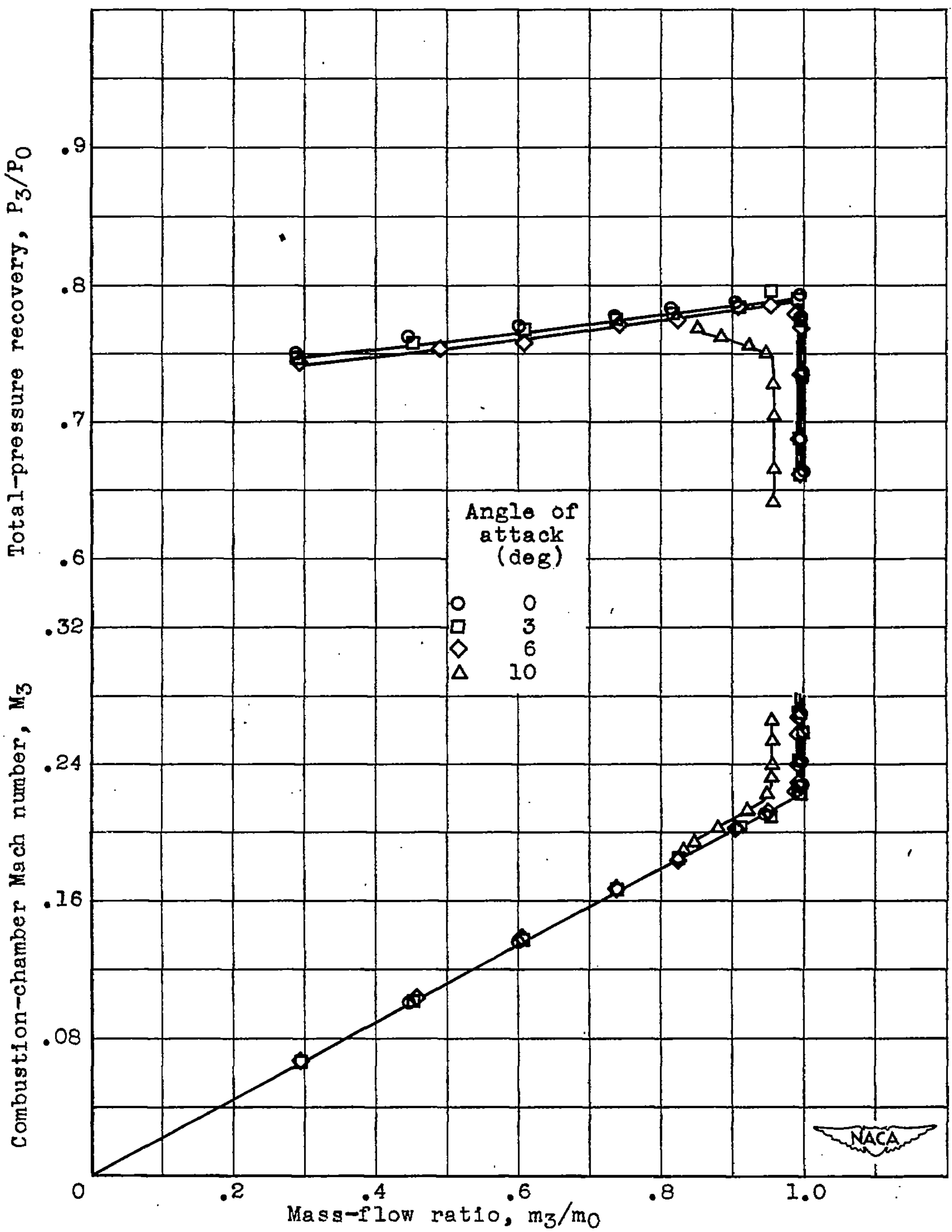

(c) Free-stream Mach number, 1.99.

Figure 25. - Concluded. Variation of total-pressure recovery and combustion-chamber Mach number with mass-flow ratio at four angles of attack for three Mach numbers. Model B.

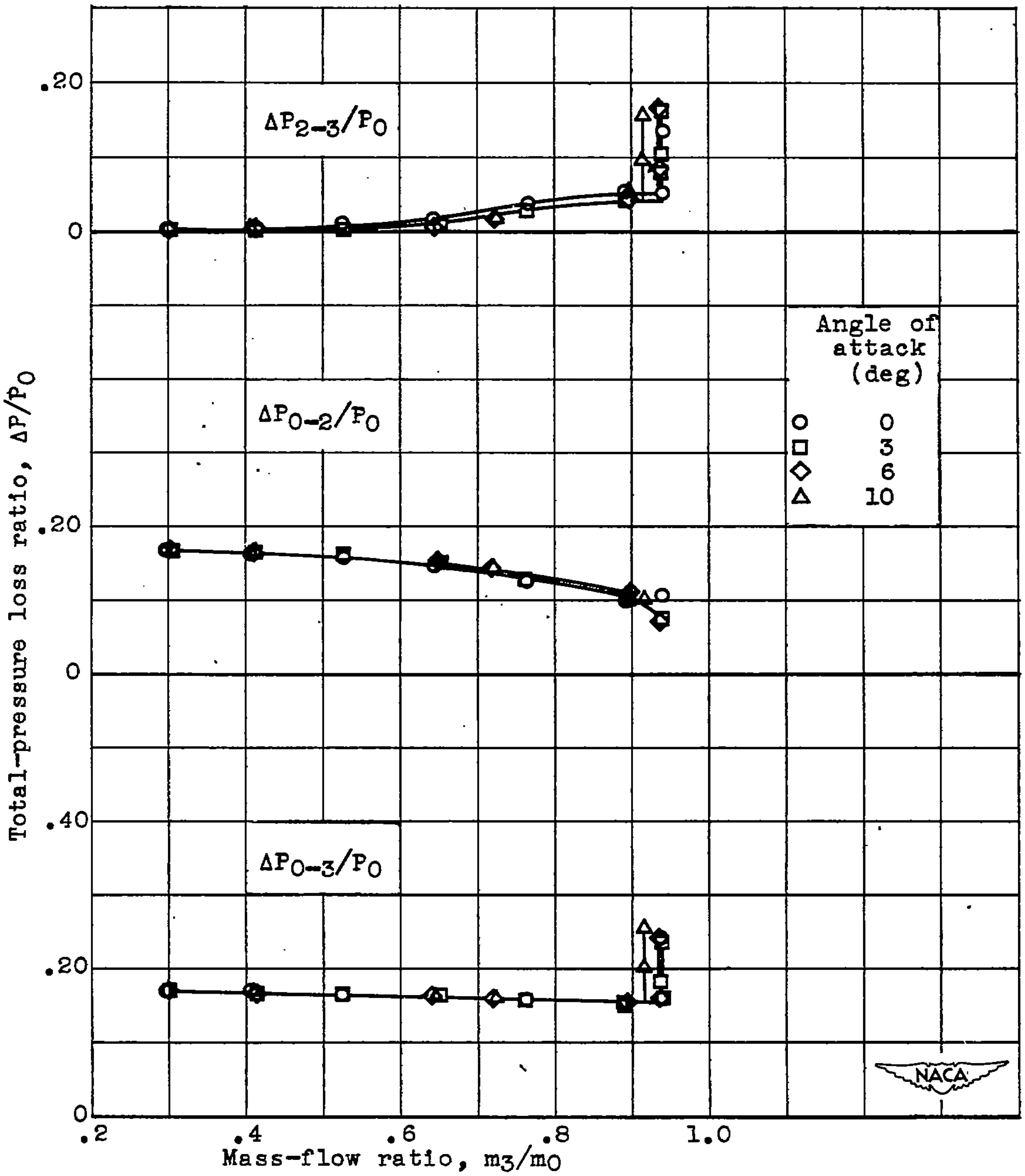

Figure 26. - Variation of inlet and subsonic-diffuser losses with mass-flow ratio at four angles of attack. Free-stream Mach number, 1.79.

NACA-Langley - 2-14-51 - 495